AN EFFICIENT NUMERICAL SCHEME FOR SIMULATING UNIDIRECTIONAL IRREGULAR WAVES BASED ON A HYBRID WAVE MODEL

A Thesis

by

DONGXING JIA

Submitted to the Office of Graduate Studies of
Texas A&M University
in partial fulfillment of the requirements for the degree of

MASTER OF SCIENCE

Approved by:

Chair of Committee,	Jun Zhang
Committee Members,	Moo-Hyun Kim
	David A. Brooks
Head of Department,	John M. Niedzwecki

December 2012

Major Subject: Ocean Engineering

ABSTRACT

The Unidirectional Hybrid Wave Model (UHWM) predicts irregular wave kinematics and pressure accurately in comparison with its linear counterpart and modification, especially near the free surface. Hence, in using the Morrison equation it has been employed in the computation of wave loads on a moored floating structure, such as Spar or TLP (Tension Leg Platform), which can be approximated by a slender body or a number of slender components. Dr. Jun Zhang, with his former and current graduate students, have developed a numerical code, known as COUPLE, over the past two decades, simulating 6 Degree Of Freedom (DOF) motions of a moored floating structures interacting with waves, current and wind. COUPLE employs UHWM as a module for computing wave loads on a floating structure. However, when the duration of simulating the wave-structure interaction is long, say 3 hours (typically required by the offshore industry for extreme storm cases), the computation time of using UHWM increases significantly in comparisons with the counterpart based upon linear wave theory.

This study is to develop a numerical scheme which may significantly reduce the CPU time in the use of UHWM and COUPLE. In simulating irregular (or random) waves following a JONSWAP spectrum of a given cut off frequency, the number of free wave components in general grows linearly with the increase of the simulation duration. The CPU time for using a linear spectral method to simulate irregular waves is roughly proportion to N^2, where N is the number of free wave components used in simulating

irregular waves, while that for using a nonlinear wave model, such as UHWM, it is roughly proportional to N^3. Therefore, to reduce the CPU time, the total simulation duration is divided into a number of segments. However, due to the nature of Fast Fourier Transform (FFT), the connection between the two neighboring surface elevations segments is likely discontinuous. To avoid the discontinuity, an overlapped duration between the two neighboring segments is adopted. For demonstration, a free-wave spectrum is input to COUPLE for simulating the 6 DOF motions of a floating 5-MW wind turbine installed on an OC3 moored Spar and tensions in the mooring lines. It is shown that the CPU time for the above simulation for duration of 2048 seconds is reduced from more than16 hours when the irregular wave elevation and kinematics are calculated without dividing into segments to less than three hours when those are calculated by dividing into five segments.

ACKNOWLEDGEMENTS

I would like to thank my committee chair, Dr. Jun Zhang, and my committee members, Dr. Kim and Dr. Brooks, for their guidance and support throughout the course of this research. They are really professional and nice. It is an honor that I have the chance to study with them which is truly a precious experience in my life.

Mr. Cheng Peng has given me a lot of support and advice throughout the research and especially in the application part of the thesis.

Thanks also go to my classmates and the department faculty and staff for making my time at Texas A&M University a great experience.

Finally, thanks to my mother and father for their encouragement and financial support. Great thanks to my wife. She is so brave and selfless during raising our first child. All my love to her, she means very much to me.

NOMENCLATURE

CG	Center of Gravity
FAST	Fatigue Aerodynamics Structures and Turbulence
FFT	Fast Fourier Transform
JONSWAP	Joint North Sea Wave Project
IFFT	Inverse Fast Fourier Transform
TLP	Tension Leg Platform
UHWM	Unidirectional Hybrid Wave Model
C_M	Modification Coefficient
df	Basic frequency increment
dt	Time step
H_s	Significant Wave Height
T_p	Peak Period

TABLE OF CONTENTS

LIST OF FIGURES

LIST OF TABLES

Page

1. INTRODUCTION

1.1 Introduction of the UHWM

Unlike in the laboratories, surface elevations cannot be readily measured in the ocean, for this reason, they are often indirectly measured using pressure transducers, velocity meters or other instruments due to the cost of deployment and severe sea environment. Even if the surface elevation is directly measured, wave-induced kinematics or dynamic pressure for the computation of wave loads on structures or wave-induced material transport still need to be determined. Hence, for the application in the offshore and coastal engineering field, the simulation of irregular waves has always been a key part. A lot of software and programs have been developed based on different wave models and theories. My study focuses on the efficiently simulating scheme of the Unidirectional Hybrid Wave Model (UHWM) theory.

Ocean waves are usually modeled as the superposition of many basic wave components (known as free or linear wave components) with different amplitudes, frequencies and phases, and together with their nonlinear interactions. Current engineering practices often use the linear spectral method to estimate irregular wave properties. In such a method, the effects of nonlinear wave interactions are ignored in the decomposition of a measured wave field using Fast Fourier Transform (FFT). When the ocean waves are not steep, the free-wave components are dominant in almost entire frequency range, and then linear spectral methods might offer a fairly good approximation. When the waves are steep, the free-wave components remain dominant near the spectral peak frequency but the bound-wave components (which describe the

effects of the strong interactions among free-wave components) may become dominant or comparable to the free-wave components in the frequency ranges either much lower or higher than the peak frequency (Zhang et al. 1996). Therefore, in this case, the ignorance of bound-wave components in linear spectral methods may result in large discrepancies. For accurate prediction, nonlinear wave effects have to be considered.

UHWM considers nonlinear effects of wave-wave interactions on the resultant wave elevations, kinematics and pressure. In the model, only strong interactions (which are noticeable after the duration of about one dominant wave period) are considered while weak interactions are ignored. Because for the purpose of predicting wave properties in a short distance, like a few wave length of the dominant wave component, weak interactions are insignificant and can be neglected.

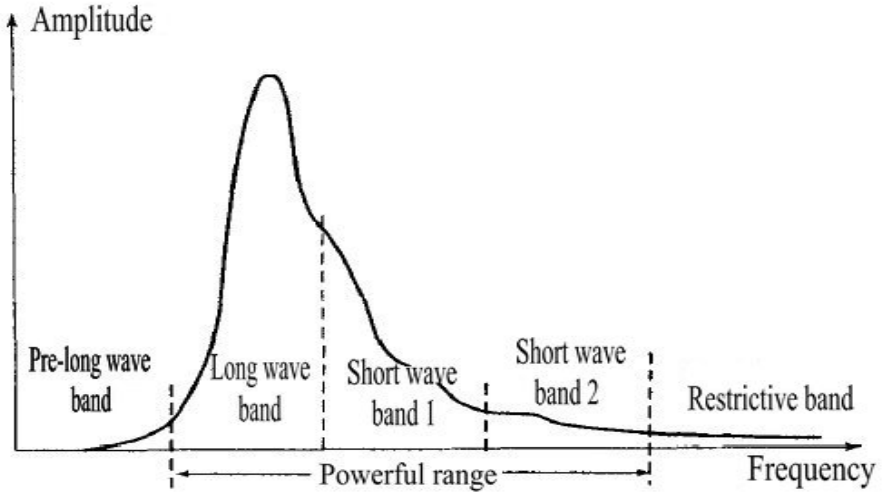

Figure 1. Sketch of JONSWAP Spectrum Band Division.

The JONSWAP (JOint North Sea WAve Project) spectrum is applied to simulate wave elevations in the UHWM and usually divided into three regions: a very low frequency region (pre-long wave band), a ‘Powerful’ region, a very high frequency region (restrictive band), as sketched in the Figure 1. Because the components located in the very low or high frequency regions are of relatively small amplitude or steepness, any interactions involving wave components in either regions are not significant which can be ignored for simplifying the computation. The ‘powerful’ region is further divided into three bands: the long-wave band, the short-wave band 1 and 2, as showed in Figure 1.

The capital letter ‘H’ in the UHWM, stands for ‘hybrid’ which refers to selectively using the conventional perturbation and phase-modulation approaches to address nonlinear interactions at the second order between two free-wave components based on their frequency ratios. The conventional perturbation approach is used for modeling interactions between two wave components with close frequencies, which are in the same band. The phase modulation approach is used for the interaction between two wave components of quite different frequencies, and they in general are located in different bands. It is known that the solution of interactions between two wave components with quite different frequencies using the conventional approach, when truncated at second order, may not converge because of the use of a linear phase function to describe the strongly modulated short-wave phase (Zhang et al. 1993). The subtraction of the nonlinear wave effects from the measured wave properties is conducted in the order from low to high on the bands. Finally, the free-wave components

are obtained by iteratively decoupling the free-wave components and their nonlinear interactions.

The nonlinear effects can be deterministically decomposed by the hybrid wave model which can not be completed by other known software. On the other hand, some certain disadvantages exist. The biggest one is: if the simulation duration (which refers to the period length of a non-repeatable wave train) is very long, it takes too much time to obtain results. Roughly speaking, in simulating irregular (or random) waves based on a spectrum of a given cut-off frequency, the number of free wave components grows linearly with the increase of the simulation duration and the CPU time for using a linear spectral method to simulate irregular waves is roughly proportion to N^2, where N is the number of free wave components that used in simulating irregular waves. However, that for using a nonlinear wave model, such as UHWM, is roughly proportional to N^3. Hence, as N grows, the CPU time grows much more significantly than the use of linear spectral methods.

1.2 DECOMPOSITION and PREDICTION

There are two main modules named DECOMPOSITION and PREDICTION in the UHWM. Just as their name implies, DECOMPOSITION decomposes an irregular wave elevation time series (or pressure, or kinematics) that were recorded either from real ocean field or laboratory, or predicted by the PREDICTION module of UHWM. The output of DECOMPOSITION is the free-wave components irregular wave train in the form of frequency/amplitude/initial phase. During the decomposition, the nonlinear wave effects are decoupled at least to second order of wave steepness. PREDICTION predicts the nonlinear wave elevations (or velocity and acceleration or pressure) based on the free-wave amplitude spectrum and initial phase. In the previous research and industry application, these two modules have proved to be robust.

Below is an example of using UHWM. Given the significant wave height Hs =5m, Peak period Tp =10s and apply the formulation below (Goda, 1987).

$$S(f) = \beta_J H_{1/3}^2 T_p^{-4} f^{-5} \exp[-\frac{5}{4}(T_p f)^{-4}]\gamma^d \qquad (1 - 1)$$

where $\beta_J = \frac{0.06238}{0.230 + 0.0336\gamma - 0.185(1.9+\gamma)^{-1}}[1.094 - 0.01915\ \mathrm{In}\gamma]$

$$d = \exp[-\frac{(f / f_p - 1)^2}{2\sigma^2}]$$

$$f_p = \frac{1}{T_p}, \quad \gamma(\text{sharp factor}) = 1 \sim 7(\text{mean } 3.3),$$

$$\sigma = \begin{cases} 0.07 & f \le f_p \\ 0.09 & f > f_p \end{cases}$$

In this example, the simulation duration T=512s, and the basic frequency increment is determined to $df = \frac{1}{T} = \frac{1}{512} s^{-1}$. The cut-off frequency is set at 0.25Hz and water depth H =1000m (to the deep water). Then the number of wave components is fixed to 128. Afterwards, discretize the corresponding JONSWAP spectrum to obtain the discrete amplitude spectrum, plus randomly select initial phase from – π to π to each wave component. Input the amplitude spectrum with random (initial) phases file to PREDICTION to generate a wave elevation time series. In order to test the consistency between these two modules, input this wave elevation to DECOMPOSITION. As mentioned at the beginning, DECOMPOSITION can remove nonlinear effects and PREDICTION can add those effects, the final result should be an amplitude spectrum that closely matched the original amplitude spectrum that was input to PREDICTION, which proves to be true, as showed in Figure 2. In the Figure 2, these actually are all discrete amplitude spectrum that discretized from its energy spectra, while for the purpose of better reveal, they are plotted continuously. From the comparison, it is clear that nonlinear effects added to the very low frequency and relative high frequency region as theory describes, plus the final amplitude spectrum and original are well matched.

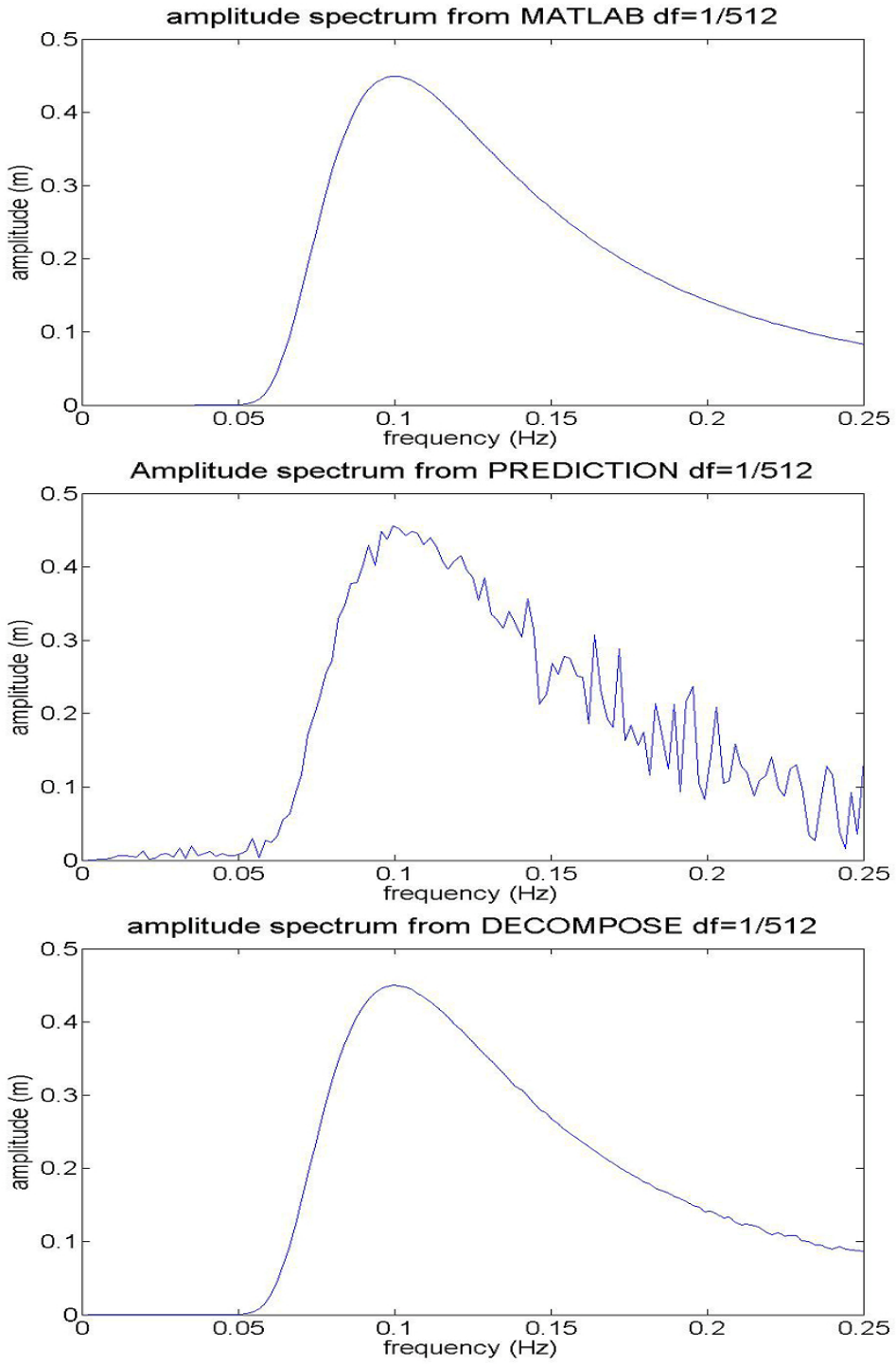

Figure 2. Comparison of amplitude spectrum (Top - Origin amplitude spectrum from Matlab; Middle - amplitude spectrum from PREDICTION; Bottom - amplitude spectrum from DECOMPOSITION).

1.3 The discontinuity

For this UHWM model, when the simulation duration is long, the CPU time rises significantly. To reduce the CPU time, it had been tried to divide the wave time series into several segments and simulate each individually. All segments have the same discrete amplitude spectrum but different initial phases. However, the wave properties, including wave elevations are discontinuous at the connection of the two neighboring segments. Another attempt is to divide a continuous time series into several segments and inversely to decompose each of them into related wave amplitude spectra and initial phases. Therefore, effectively reduces the number of free wave components and hence the CPU time. Nevertheless, the connection between two neighboring segments may not be continuous. In other words, the wave elevations, kinematics and pressure may disrupt at the connection point between two neighboring segments. This is because, by nature of the IFFT (Inverse Fast Fourier Transform) assumes each segments is periodic in time domain. When a free-wave amplitude and phase spectrum decomposed band upon a segment taken from a longer continuous time series, it may not exactly recover the segment at the beginning and end due to well- known Gibbs phenomenon. It involves both the fact that the sums of Fourier overshoot at a jump discontinuity, and plus the overshoot does not die out as the frequency increases, as shown in Figure 3 next page (Rössel, 2010).

In mathematics, it is the peculiar manner in which the Fourier series of a piecewise continuously differentiable periodic function behaves at a jump discontinuity: the n^{th} partial sum of the Fourier series has large oscillations near the jump, which might

increase the maximum of the partial sum above that of the function itself. The overshoot does not die out as the frequency increases, but approaches a finite limit (Carslaw, 1930). In short, such problem occurs when apply a periodic function like sine/cosine to describe a non-periodic function. Hence, if the wave time series data is simply separated, during simulation at the very moment, especially at the boundary points of segments, the 'jump' point would take place and cause discontinuity problem. Clearly, our effect is to find out a scheme that fulfills the FFT while also speeds up the CPU time and keep the accuracy of the simulation.

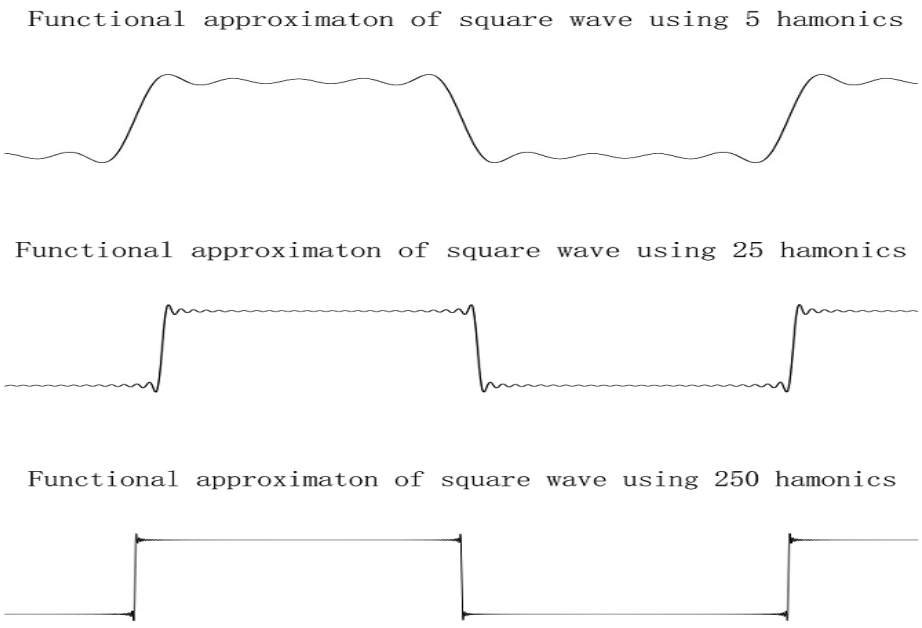

Figure 3. Gibbs phenomenon of functional approximation of square wave using three different harmonics.

2. METHODOLOGY: EFFECTIVE OVERLAP SCHEME

2.1 JONSWAP spectrum modification

A JONSWAP (JOint North Sea WAve Project) spectrum describes the distribution of wave energy at different frequencies (Stewart, 2005). It is derived from actual ocean wave measurements and the measured wave elevation is the resultant wave elevation which always includes both of free-wave and bound-wave elevation. However, PREDICTION predicts the resultant wave elevations based on free-wave components only. Hence, it is appropriate to modify a JONSWAP spectrum to eliminate the contribution from bound-wave components.

The modification of a JONSWAP spectrum to eliminate the contribution of bound-wave components is based on the nominal wave steepness ($H_s \times k_p /2$), peak frequency σ_P or peak period T_P and the cut-off frequency σ_c. In this study, the computation of the peak wave number (k_p) is based on deep-water assumption. It is known the wave steepness is proportional to the amplitude, at the same time, the energy density is proportional to the square of amplitude, so the wave steepness is set in the squared form to be better corresponded to the change rate of energy. Secondly, the modification region should be carefully chosen. According to the phase modulation theory, the nonlinear effects play roles mainly in the very low frequency and relatively high frequency regions. While at the very beginning of the spectrum, the energy is virtually zero and no modification is necessary. Hence, the modification region is located somewhere behind the peak and to the cutoff frequency. After several tests, the

ratio of T_p and T_c equal to 3 is used, where T_c is the cutoff period. Based on the UHWM theory, the nonlinear wave effects mainly play roles in the relatively high frequency region, therefore, pick the modification region between 1.35 and 3 times of peak frequency, the results of PREDICTION wave energy density are identical to those of the corresponding JONSWAP.

About the modification region, it is worth noting that, the starting and end points should be fixed to the same frequency no matter the simulation durations are different, in order to obtain the consistent results. For example, for $H_s = 12m / T_p = 12s$, simulation duration 512 s case, fix the beginning point of the modification region at 58th point (58= 59-1, this "minus 1" indicates the first direct current component in the spectrum which should be removed from the calculation). Hence, under the same sea state but simulation duration equal to 1024 s case, although the number of components grows twice, in order to keep the beginning point of modification region at the same position, such point is fixed at 117= (59*2)-1. Similarly, for simulation duration 2048 s case, it is 235= (59*4)-1, where all follow the equation ($59*2^n$)-1 to further cases.

Based on the trial and error approach, the final modification equation is given, where α is an adjusted coefficient equal to 0.45.

$$C_{Modify} = \alpha \times (\frac{H_s^{\ 2}}{T_p^{\ 4}} \times \frac{16\pi^4}{g^2}) \times (\frac{T_p}{T_c}) \qquad (2 - 1)$$

And such coefficient is used in the form of:

$$a'_{(n)} = a_{(n)} \times (1 - C_M \times \frac{n - N_{Mod}}{N_{Cut} - N_{Mod}}) \qquad (2 - 2)$$

where $a'_{(n)}$ and $a_{(n)}$ are the amplitude at different frequencies in the modified and original discrete amplitude spectrum; N_{Mod} is the number of first point where the modification starts and N_{Cut} is the number of cut-off frequency point; n is a variable that grows from N_{Mod} to the number of cut-off frequency. Hence, after applying this, the value in the brackets varies from 1 (max value, when n= N_{Mod}) to (1 - C_M) (min value when n= N_{Cut}). Plus, the sketch of the effect of modification to discrete amplitude spectra is given below in the Figure 4. On the right is the modified area that would be removed from an original spectrum for the consistence and simplicity in the calculation.

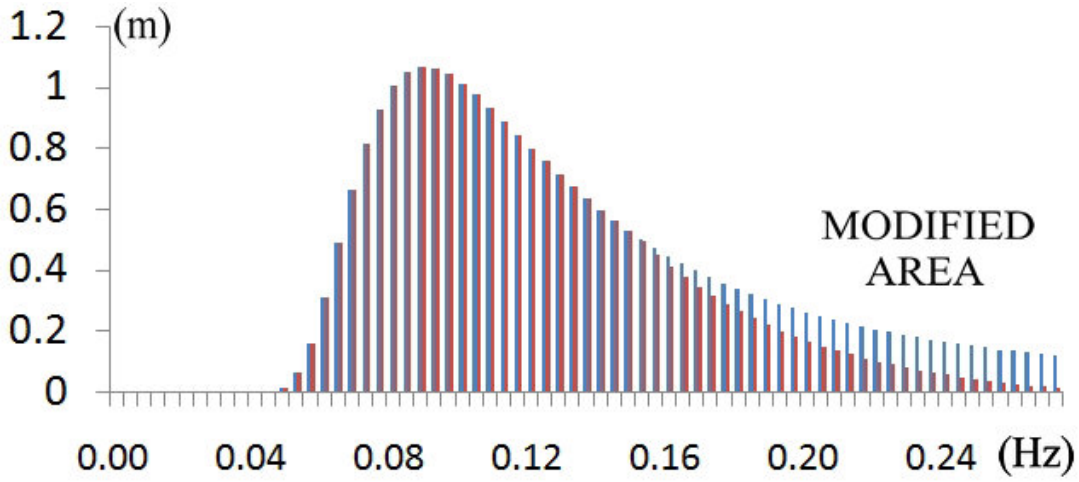

Figure 4. Sketch of JONSWAP spectrum modification.

The “tail band” described in the PREDICTION is well worth discussing. Generally speaking, the whole effective frequency region is divided into five bands: pre-long wave band, long wave band, short wave band one, short wave band two and tail band. In the fifth band, at very high frequency area, nonlinear effects play much more important role even after the cutoff frequency. The predicted resultant wave energy involves the energy in the tail band. In the Table1, the last two columns give the amount and percentage of energy of tail band. Table1 describes the results of the modified and added energy in the spectrum of different wave cases and different simulation duration. The first column is the simulation duration of each wave data, the second shows the total energy involved in a JONSWAP spectrum from the zero frequency to the cutoff frequency; the third and fourth columns are the amount of energy and related percentage of the modified JONSWAP spectrum (corresponding the related free-wave energy); the fifth and sixth columns show the amount of energy and percentage of the resultant wave energy predicted based on the modified JONSWAP spectra. Obviously, energy of waves from PREDICTION in the fifth column and that of JONSWAP spectrum in the second column matches pretty well. Table 2 shows the percentage of energy of resultant wave obtained by PREDICTION of twenty different initial phases in the comparison with the original JONSWAP spectra. While the max and min difference from JONSWAP are both around two percent, the average value of these twenty initial phase cases is 0.02%, which means the amount of energy modified by the proposed coefficient is reasonable.

Table 1(a). Comparison of energy area of original and modified and PREDICTION produced spectrum. (H_s=8m)

$H_s = 8m$	T_p=11s	$F_{cut} = 11/3s^{-1}$	$C_{Modify} = 0.0956$				
Simulation Duration (s)	JONSWAP (m^2/Hz)	Modified (m^2/Hz)		PREDICTION (m^2/Hz)		TAIL BAND (m^2/Hz)	
512	9.091	8.971	-1.31%	9.1395	**0.54%**	0.0831	0.91%
1024	9.093	8.971	-1.31%	9.137	**0.49%**	0.091	1.00%
2048	9.093	8.971	-1.31%	9.032	**0.67%**	0.0883	0.97%
4096	9.093	8.971	-1.31%	9.1149	**0.24%**	0.0846	0.93%

Table 1(b). Comparison of energy area of original and modified and PREDICTION produced spectrum. (H_s=12m)

$H_s = 12m$	T_p=12s	$F_{cut} = 0.25s^{-1}$	$C_{Modify} = 0.1519$				
Simulation Duration (s)	JONSWAP (m^2/Hz)	Modified (m^2/Hz)		PREDICTION (m^2/Hz)		TAIL BAND (m^2/Hz)	
512	20.460	20.033	-2.04%	20.5196	**0.29%**	0.2683	1.31%
1024	20.460	20.033	-2.04%	20.488	**0.13%**	0.2262	1.11%
2048	20.460	20.033	-2.04%	20.378	**0.40%**	0.2366	1.16%
4096	20.460	20.033	-2.04%	20.3659	**0.46%**	0.2604	1.27%

Table 2. Comparison of energy amount of 20 different initial phases.

T=1024s H_s=12m T_p=12s $C_{Modify} = 0.1519$							
	JONSWAP (m^2/Hz)	Modified (m^2/Hz)		PREDICTION (m^2/Hz)		TAIL (m^2/Hz)	
phase1	20.460	20.033	-2.04%	20.6044	0.71%	0.2636	1.29%
phase2	20.460	20.033	-2.04%	20.6925	1.14%	0.2231	1.09%
phase3	20.460	20.033	-2.04%	20.4652	0.03%	0.2123	1.04%
phase4	20.460	20.033	-2.04%	20.4898	0.15%	0.2776	1.36%
phase5	20.460	20.033	-2.04%	20.5857	0.62%	0.2891	1.41%
phase6	20.460	20.033	-2.04%	20.2183	-1.18%	0.2374	1.16%
phase7	20.460	20.033	-2.04%	20.3269	-0.65%	0.2753	1.35%
phase8	20.460	20.033	-2.04%	20.1796	-1.37%	0.2902	1.42%
phase9	20.460	20.033	-2.04%	20.5591	0.49%	0.2465	1.20%
phase10	20.460	20.033	-2.04%	20.2668	-0.94%	0.2707	1.32%
phase11	20.460	20.033	-2.04%	20.0624	**-1.94%**	0.2244	1.10%
phase12	20.460	20.033	-2.04%	20.3835	-0.37%	0.2754	1.35%
phase13	20.460	20.033	-2.04%	20.5988	0.68%	0.2455	1.20%
phase14	20.460	20.033	-2.04%	20.5815	0.60%	0.2554	1.25%
phase15	20.460	20.033	-2.04%	20.3974	-0.30%	0.287	1.40%
phase16	20.460	20.033	-2.04%	20.4039	-0.27%	0.2331	1.14%
phase17	20.460	20.033	-2.04%	20.4602	0.00%	0.2761	1.35%
phase18	20.460	20.033	-2.04%	20.7727	1.53%	0.2705	1.32%
phase19	20.460	20.033	-2.04%	20.3368	-0.60%	0.2656	1.30%
phase20	20.460	20.033	-2.04%	20.8804	**2.06%**	0.2792	1.36%
			Average	20.4633	0.02%	0.2599	1.27%
			Var	0.0415			

2.2 Segment division

Among several existing limitations and disadvantages of the UHWM, the biggest one is consuming too much time to obtain results if the simulation duration is too long. For example, given a simulation duration of three hours (typically required by the offshore industry for extreme storm cases); its basic frequency is fixed to 1/10800 Hz. Even if we set the cut-off frequency at 0.3Hz, there are still 3240 free (linear) wave components involved in the simulation. To the second order, take the nonlinear wave-wave interaction into account when applying the UHWM theory, the computation of wave-wave interaction rapidly increases to the square of 3,240. That is the reason why the simulation duration significantly rises, which is too long to afford.

To reduce the CPU time, a naïve attempt was previously made to divide wave elevation time series into several segments with equal length and simulate them sequentially. If we take a JONSWAP spectrum-generated, cut-off frequency at 0.3Hz, simulation duration 10800 s wave as an example, divide the wave elevation time series into ten segments, that is, for each one $T^{'} = 1,080s$. In this way, for the second order nonlinear interaction, the calculated quantity would reduce from 3240^2 to 10×324^2.

Such an approach is somehow effective to reduce the CPU time; however, at the same time it may induce discontinuity at the connection between two neighboring segments as mentioned in the introduction part. The discontinuity in wave elevation also results in discontinuity in wave kinematics and pressure, which may result in ‘jump’ in wave loads and cause non-convergent results in computation of wave-structure interactions.

2.3 Overlap region

An effective approach is developed to overcome the Gibbs phenomenon at the connection of two neighboring segments. To avoid the discontinuity, an overlap time duration between two neighboring segments is required. Since the discontinuity due to Gibbs phenomenon occurs near the connection, an overlap time duration allows the simulation to stop at the middle of overlap duration which is before the end of a segment and start at the middle of overlap region which is after the beginning of the next region. Therefore, the discontinuity at the connection is avoided, which allows smooth computation of wave elevation, kinematics and pressure.

Here is an example for the explanation of the overlap approach. Divide the total simulation duration 512 s into five segments, each segment is of 128 s duration and overlap time duration between the two neighboring segments is 32 s. Then calculate the amplitude spectra and their initial phases of each segment one by one using DECOMPOSITION. Afterwards, in order to testify the consistency, input these free-wave spectra and related initial phases to PREDICTION to obtain corresponding wave elevation times series again and recover wave elevation with the long-time duration. Since the results of two modules are consistent, it is proved that these modules are consistent.

Here is an example to show that two modules are consistent. First, the JONSWAP spectrum with H_s =5 m, T_p =10 s, $df = \frac{1}{512} s^{-1}$ is discretized to obtain the discrete amplitude spectrum. They are input to PREDICTION, where a simulation

duration equal to 512 s wave elevation time series is produced. In order to better correspond the FFT/IFFT scheme, it is required to take the number of total points in each segment equal to 2^N. In this case, N=7 (2^7=128) is chosen, plus, the time step is 1s, artificially we set 0 s to 127 s of the time series as the first segment. Then, apply the "effective wave overlap" approach, the tricky part is setting the second section to begin at 128-32=96 s (32 comes from 128/4, which is that "overlap region" mentioned before) rather than at 128 s, and ends at 223 s. For the third, again starts at 224-32=192 s instead of 224 s, ends at 319 s. Repeat this method to the rest two segments, we could find the fifth segment ends at 511 s, as showed in the Figure 5**.** Basically, if the wave elevation time series is divided into segments with equal length, say in this case 512 s/4=128 s for each section, the length of overlap region might be determined as the length of each equal segment (128 s) divide by the number of regular segments (4), that is 128 s/4=32 s. Next step input these five segments to DECOMPOSITION to obtain five amplitude spectrum and the related initial phases files. In order to promise all data are correct and consistent. These five spectral files are input to PREDICTION once more to obtain wave elevation time series of five segments and the consistency is examined by reconnecting these segments. To reconnect them, the effective overlap approach is applied, again. The detail is, for the first segment picking the last point ends at 111 s, which is the midpoint of the actual ending of section one (127 s) and the starting point of section two (96 s), by which we artificially remove discontinuous points located at the beginning and end area of each segments. For the second segment, set the starting point at 111 s+1 s=112 s

which is located in segment two and the last point at 207 s which is the midpoint of 223 s (end of this segment) and 192 s (starting of next segment).

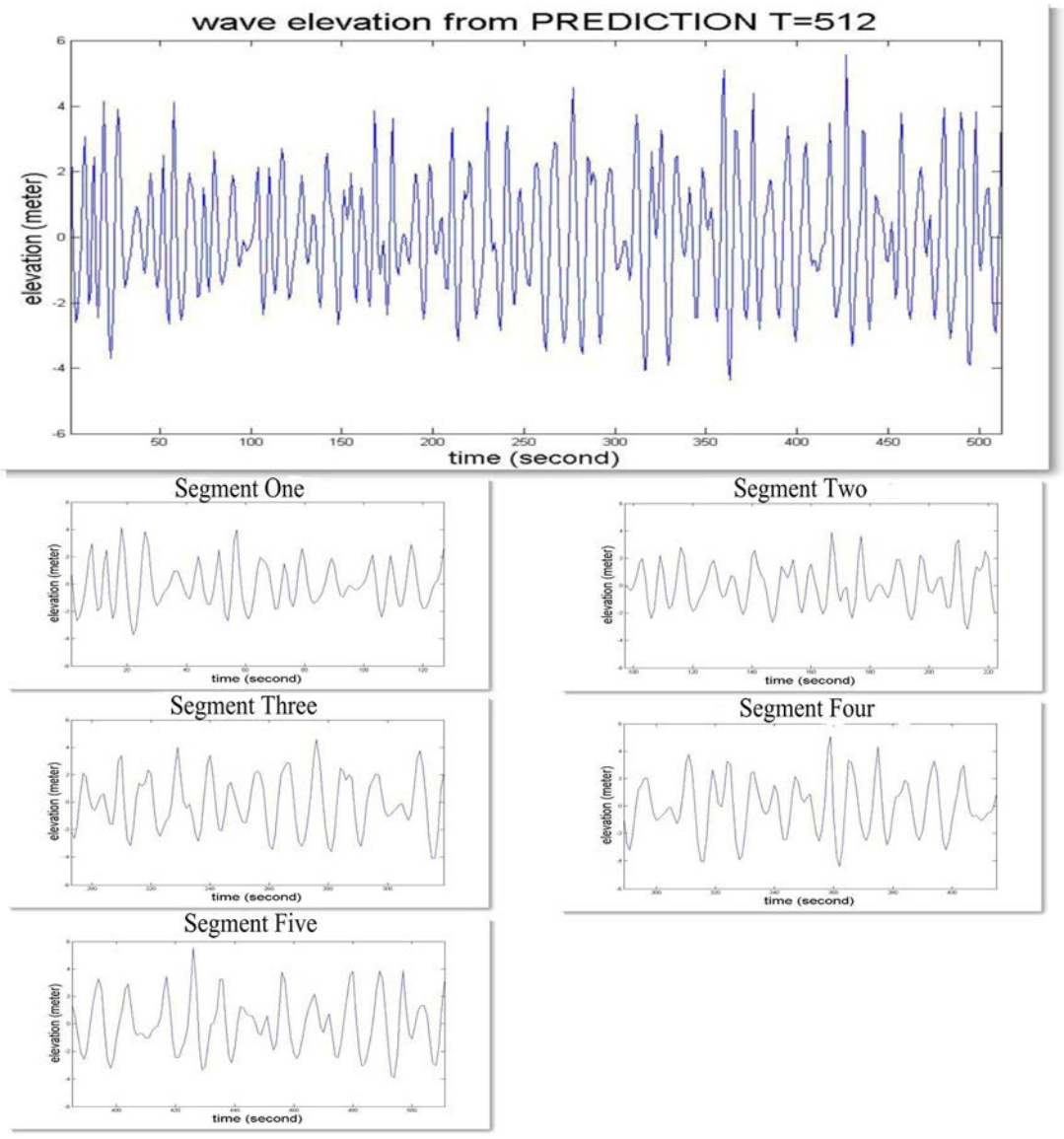

Figure 5. T=512 seconds wave elevation and five separated segments.

Figure 6 below is a sketch of how to recover the wave elevations of segments by effective approach. The thicker lines in two upper figures are effective for reconnecting waves belonging to the wave segment 1 and 2, and the thinner lines are removed by "Effective overlap" approach, where the discontinuous points are located. In the lower figure, it is the wave elevation from 0 s to 208 s which is assembling by the thick lines in upper figures and obviously, they are smooth. Repeat such process to the remaining sections and all the discontinuity points could be avoided in time domain. Above all, it is smoothly consistent between each connection points in the reconnected wave.

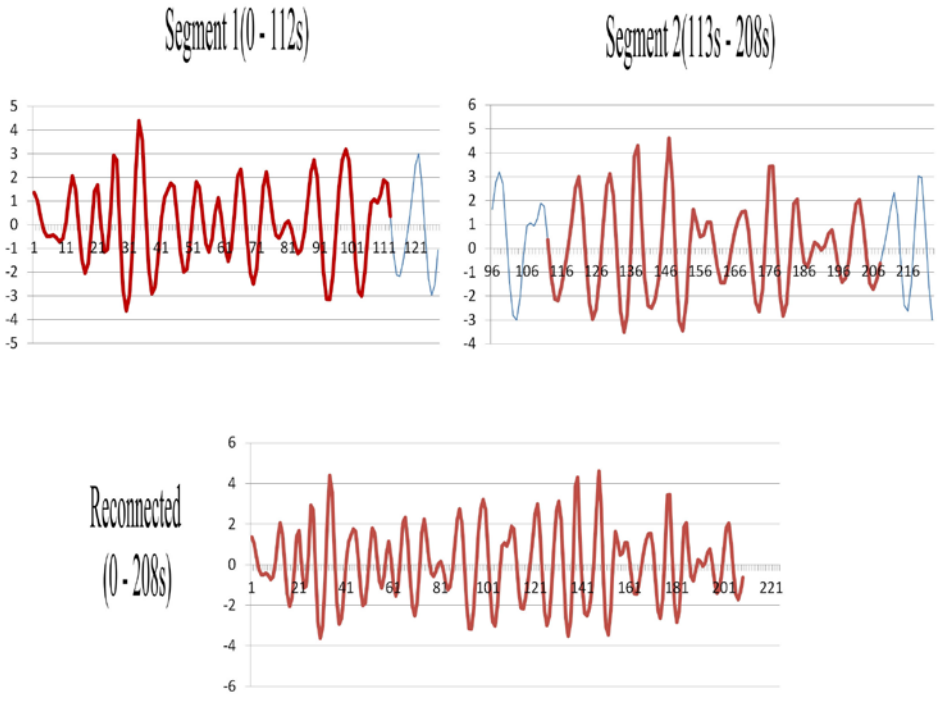

Figure 6. Sketch of how to reconnect the wave segments.

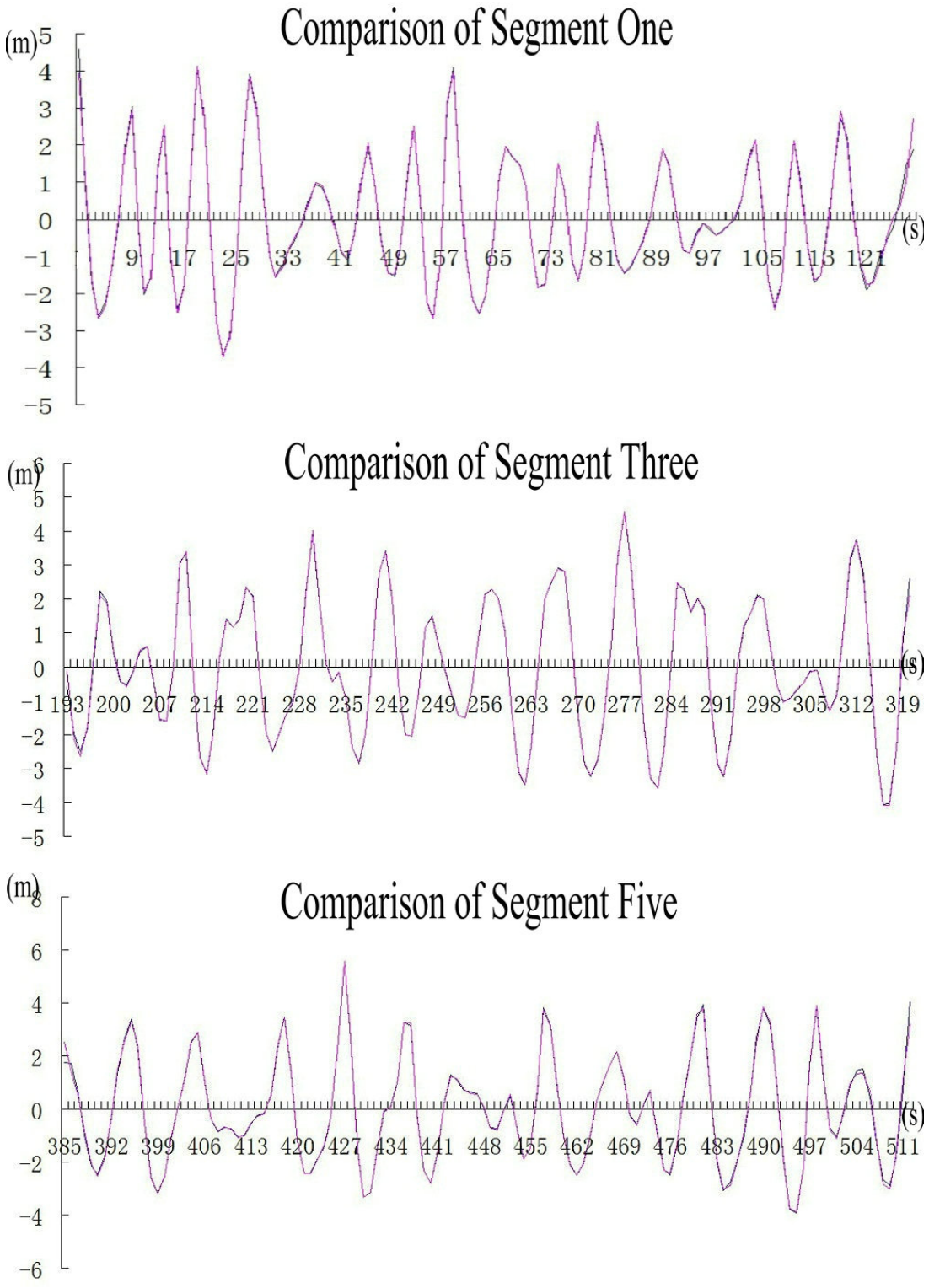

Figure 7. Comparison of segments of the first and second PREDICTION wave.

Figure 7 is the comparison of segments one, three and five, which are the output of PREDICTION based on the free wave amplitude spectra and the related initial phases with the original wave elevation time series. Apparently they well matched, except near the beginning and end of each segment. These data will be avoided when the overlapped approach is used. Figure 8 shows all four connection points between two neighboring segments. It can be observed that the dash line in the prior wave segment and the full line belonging to the following segment smoothly connected.

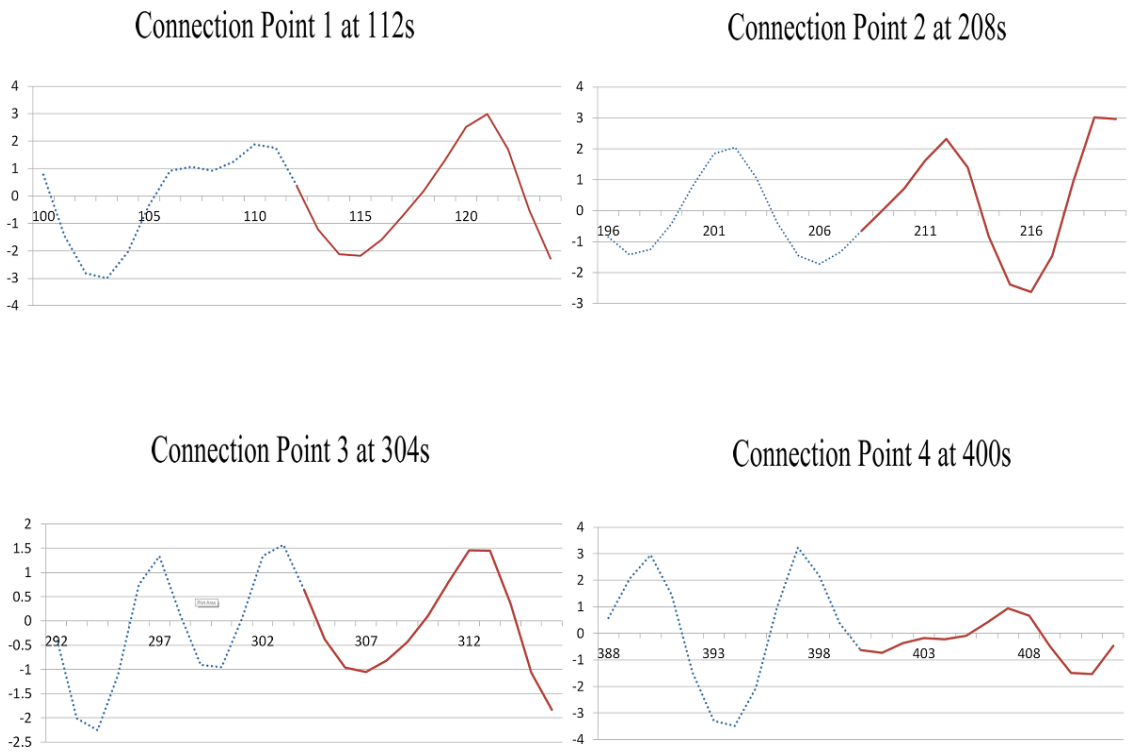

Figure 8. Four connection points of each segment (without discontinuity jump points).

3. NUMERICAL SIMULATION OF IRREGULAR WAVES

3.1 Example of generating irregular wave elevation

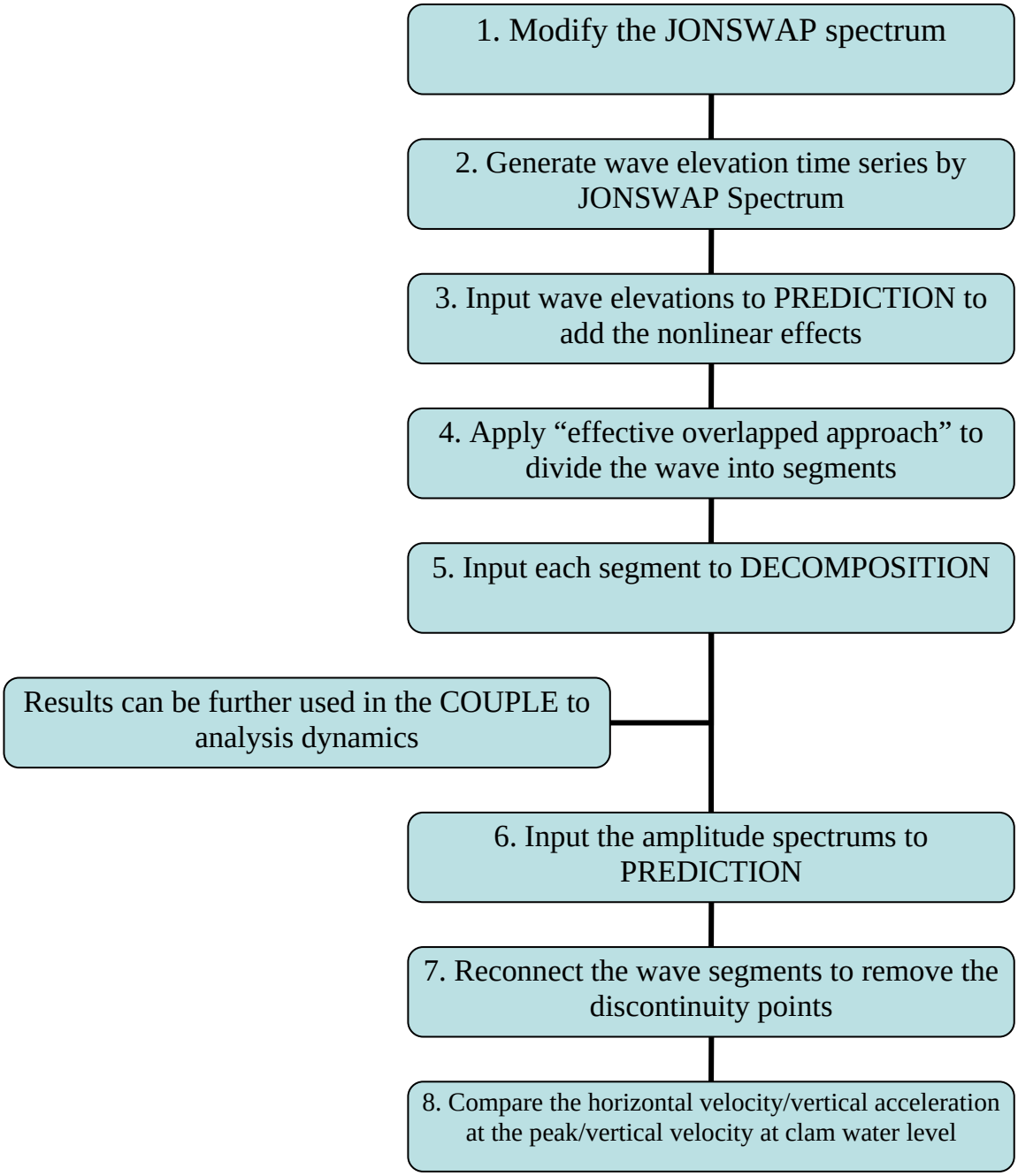

Figure 9. Flow chart of process of simulating continuous wave elevation.

This flow chart in Figure 9 provides a general view of the process of simulating the irregular wave elevation time series applying the “Effective Overlap” approach. In the thesis, above mentioned numerical scheme is used to simulate irregular waves in the case of three different sea states, namely benign sea (H_s=5 m / T_p=10 s), rough sea (H_s=8 m / T_p=11 s) and severe hurricane storm (H_s=12 m / T_p=12 s). In each sea state, the wave elevation is simulated from a simulation duration 2048 s and sample rate equal to 8 (which makes time step dt=1/8 s). Within the “Effective Overlap” approach, set the length of each segment equal to 256 s and consequently divide the wave data into nine segments, among which eight segments come from equally divided the whole data (2048/256=8) and one comes from overlap. Correspondingly, in each segment there are 256*8=2048=2^{11} points where is designed to better fit the IFFT/FFT to recover the wave elevation profiles during the simulation. Plus, nine segments give eight overlapped regions, thus the overlapped distance between every neighboring segments is determined to 256 s/8=32 s.

In the flow chart, the first, second and third steps have been described in previous sections and omitted here. The fourth step is to divide the wave elevation time series data. In particular, the first wave segment starts at 0s and end at 255.875 s rather than 256 s is worth noticing. Either the first (0 s) or the last point (256 s) could be included; otherwise there is more than 2^{11} points in one segment. Since the simulation duration is set to 256 s for each segment, the point of 256 s actually repeated to 0 s. And the second segment starts at 224 s = 256 s (next point of end of segment one) -32 s (overlap length) and ends at 479.875 s = 224 s+255.875 s rather than 480 s. For the last ninth segment, it

starts at 1792 s and ends at 2047.875 s. Then input nine segment files to DECOMPOSITION serially and the results will be further used in the COUPLE.

To make sure the consistency of the wave data generated. Steps 6, 7 and 8 are included. In the sixth step, when input these amplitude spectrum data files into PREDICTION, the band division of the spectrum is well worth highlighting to discuss, especially for the division of long-wave band in the severe hurricane storm state. Based on the UHWM theory, two criteria are imposed in the band division of the powerful range including the long wave band, short wave band 1 and short wave band 2. First, the width of each band must be narrow enough so that the truncated conventional solutions converge rapidly and it is limited to maximum equivalent wave steepness ε_e. The wave components located in long wave band all have relatively high energy which should be carefully selected. The first component of the long-wave band starts right after the very low frequency range when the amplitude of the component becomes large enough, say reaching 7% of the spectrum peak amplitude. The last component is allowed to be included in the long-wave band if the maximum equivalent wave steepness is much smaller than one, where the maximum equivalent wave steepness is

$$\varepsilon_e = k_{N_h} \sum_{j=N_1}^{J} \alpha_j a_j \sin\theta_j \qquad (3 - 1)$$

N_1, N_h are the subscriptions of the first and last wave components in the long-wave band, respectively. $\theta_j = k_j x + \sigma_j t + \beta_j$, β_j is the initial phase and in this case, set $x = 0$. By comparing the previous research, such criteria ensure rapidly convergence of the solution when the conventional approach is used (Zhang et al. 1996). The second

criterion results from the assumption made in the modulation approach where the water depth is deep with respect to the short-wave band components. The division between the long-wave band and the short-wave band 1 is examined whether or not this assumption is satisfied. Therefore, it is not appropriate to apply the present wave model to irregular waves in relatively shallow water. After several tests, it is found that the division of long-wave band in H_s=12m case is more sensitive than the others, even one more short-wave component included in the long-wave band, sometimes the result is difficult to be converge. Finally, the band division for these three cases is determined as, 11/32/53/78/115 for H_s=5m; 10/31/50/71/106 for H_s=8m; 9/22/45/65/99 for H_s=12m. These five numbers refer to the boundary points of each band and the first neighboring two refer to the boundary point of long-wave band, the second and third refer to the boundary point of short-wave band 1, the third and fourth refer to short-wave band 2, the last two refer to tail band. After the process of PREDICTION, the wave elevation files can be obtained. Compare them to the original segments; obviously, the profiles are well matched except at the boundary connected area. While this distorted region could be removed by effective overlapped approach, some specific segments have given below.

Actually, a ramp-function is applied in the COUPLE to calculate the dynamic results with simulated waves, by which the very beginning of wave elevation data is artificially ignored in order to keep the force starting to grow from zero rather than a sudden large value which is a design to better fit the real sea condition. In the Figure 9, it is the segment one of H_s=5m case. Thus, at the beginning of segment one there is no need to fix the discontinuity region. The “Effective overlap” approach is applied ever

from the ending area of the segment one at t=240s. In Figure 9, the lower profile is enlarged as the rectangle region in the upper profile. By the “Effective overlap” approach, the effective points included from 0s to t=239.875s and the rest (240s – 255.875s) are ignored. The first point of segment two will be counted from t=240s which is consistent to the prior point.

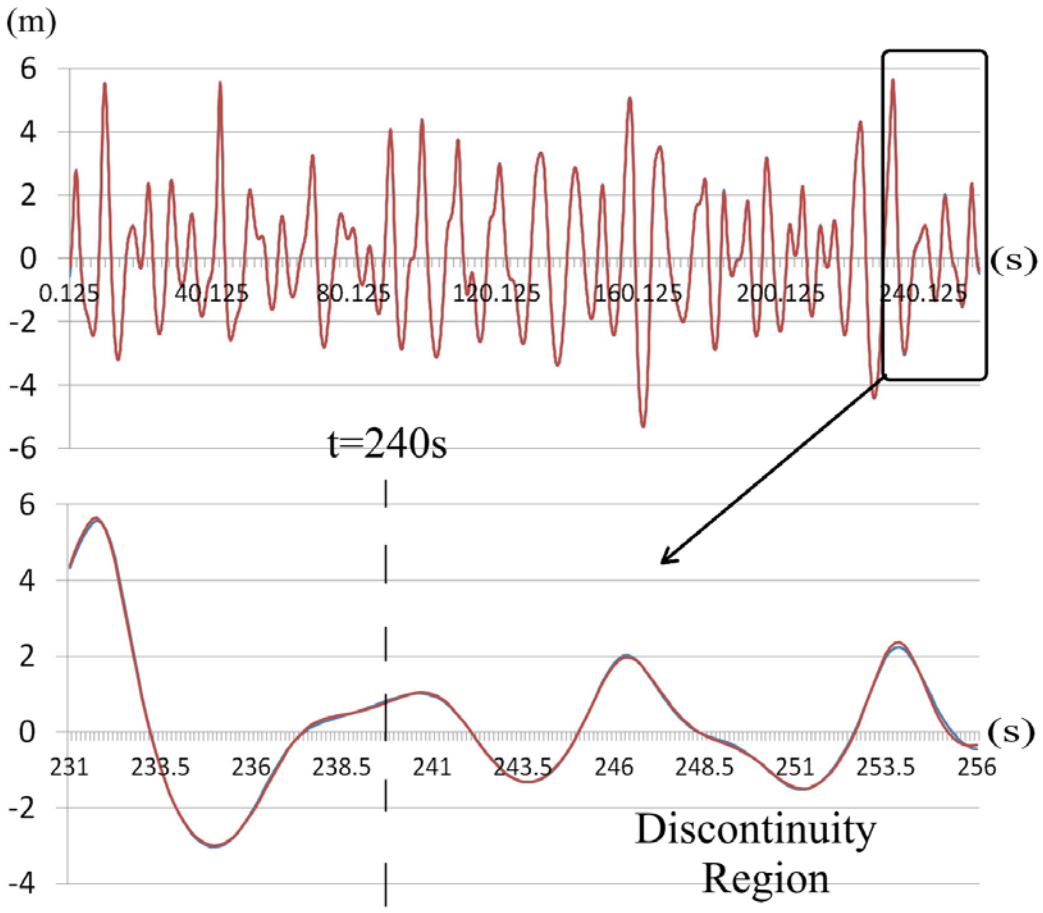

Figure 10. Wave elevation of segment 1 (Hs=5m).

Figure 10 is the segment five of H_s=8m case. As showed in the figure, both the starting and end region is modified by “Effective overlap” approach and its detail is enlarged in the rectangle area to be better understood. From the figure, it can be observed that as the significant wave height grows, the distortion also grows in the discontinuity connected area. That is why in the previous research, for the H_s=5m or 8m cases, even if we do not apply the “Effective overlap” approach to the simulated wave, failing to get the convergent results does not always happen. However, during the H_s=12m case, in almost more than half cases it is hard to obtain good result as wanted. That is the basic stimulation of developing the “Effective overlap” approach.

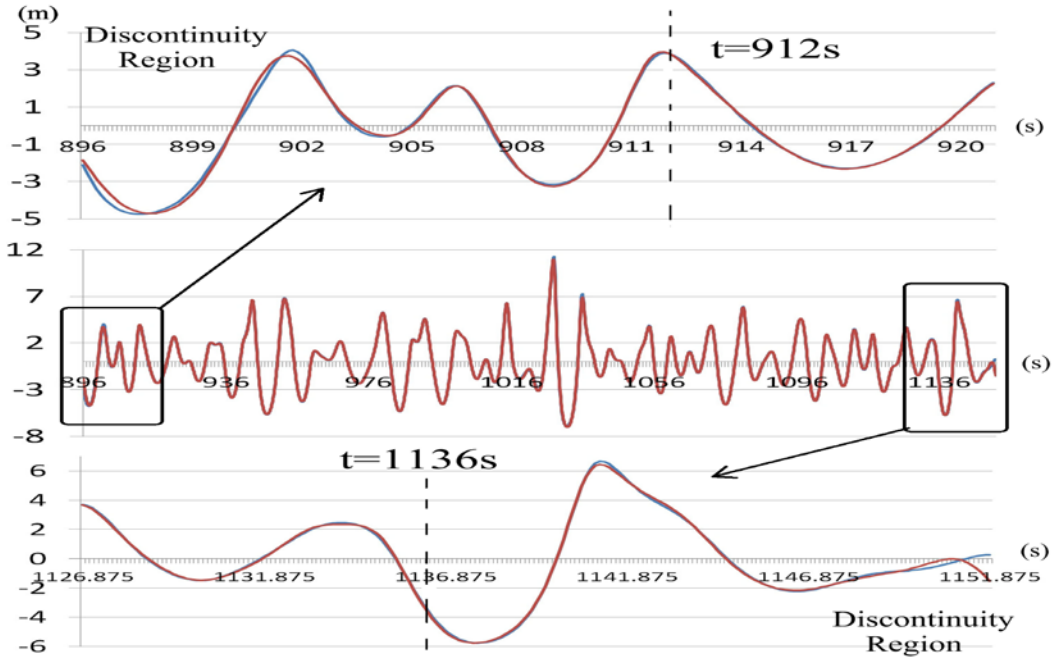

Figure 9. Wave elevation of segment 5 (Hs=8m).

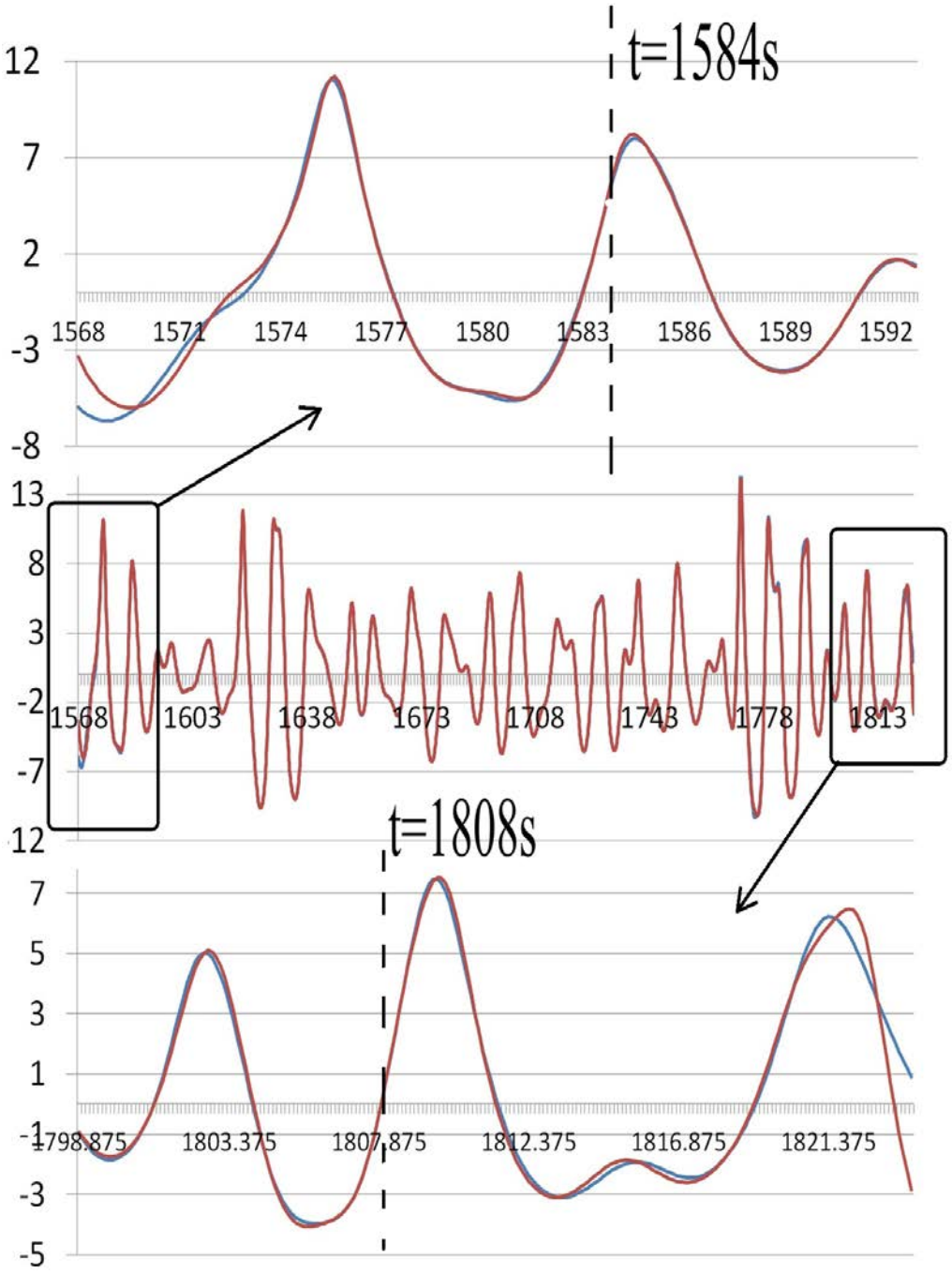

Figure 10. Wave elevation of segment 8 (Hs=12m).

3.2 Comparison of velocity and acceleration

Additionally, in order to further test the consistence of original and PREDICTION wave segments, the comparison of horizontal velocity and vertical acceleration at the peak is plotted. Since, the wave particles have relatively large horizontal velocity and vertical acceleration at the peak, thus, the difference of these two data profiles can be better revealed by the comparison. In Figures 12 – 14, the vertical coordinate is set such that the calm water level is zero and positive for position located above the calm water level and negative below. The lower coordinate of the profile is -30m and rising to the peak, plus the vertical distance increment is 0.1m for better resolution. As showed, even at the peak two profiles match each other which prove the consistency of two wave elevation.

Also, the comparison of particles vertical velocity at the intersection of the calm water level is plotted. Similarly, it is drawn in the coordinate of -30m to 0 vertically and increment equals to 0.1. One thing to mention, in Figure 15 and 17 the velocity is positive which means it is an up-going wave component. And in Figure 16, the down-going wave component makes the velocity negative. No matter it is up-going or down-going; the comparison shows that the PREDICTION wave and that after applying the "Effective overlap" scheme are consistently matched, not only in the wave elevation comparison profiles but also in the velocity and acceleration comparison profiles.

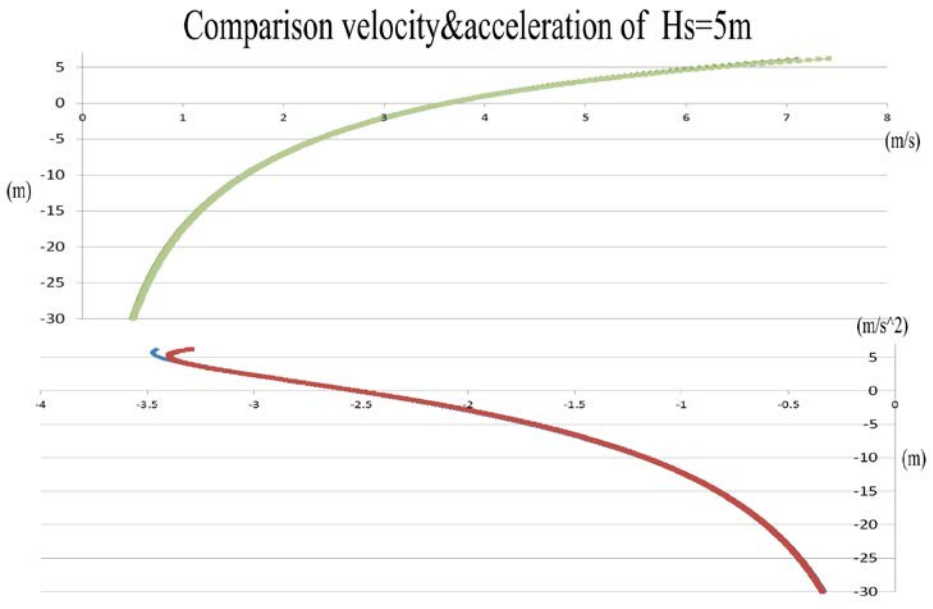

Figure 13. Comparison of horiz. velocity and acceleration at the peak (Hs=5m).

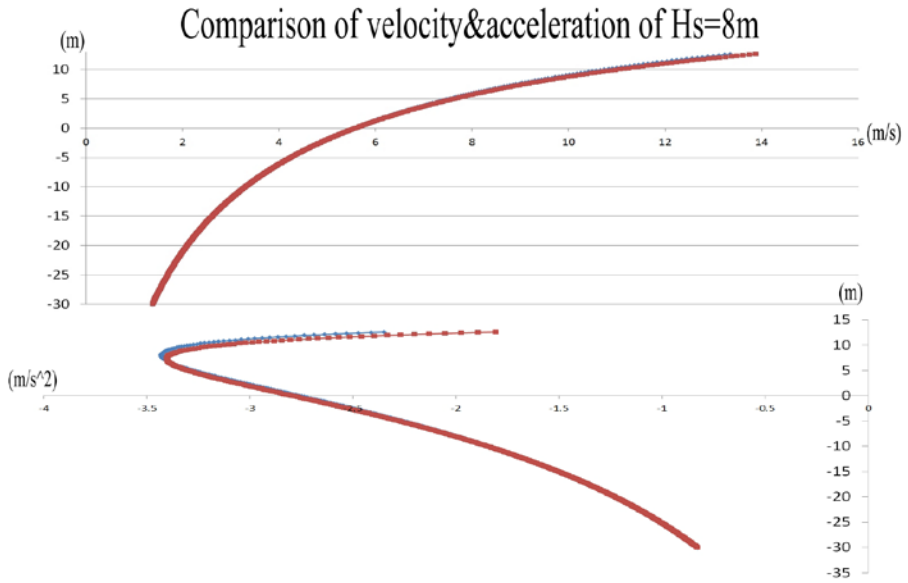

Figure14. Comparison of horiz.velocity and acceleration at the peak (Hs=8m).

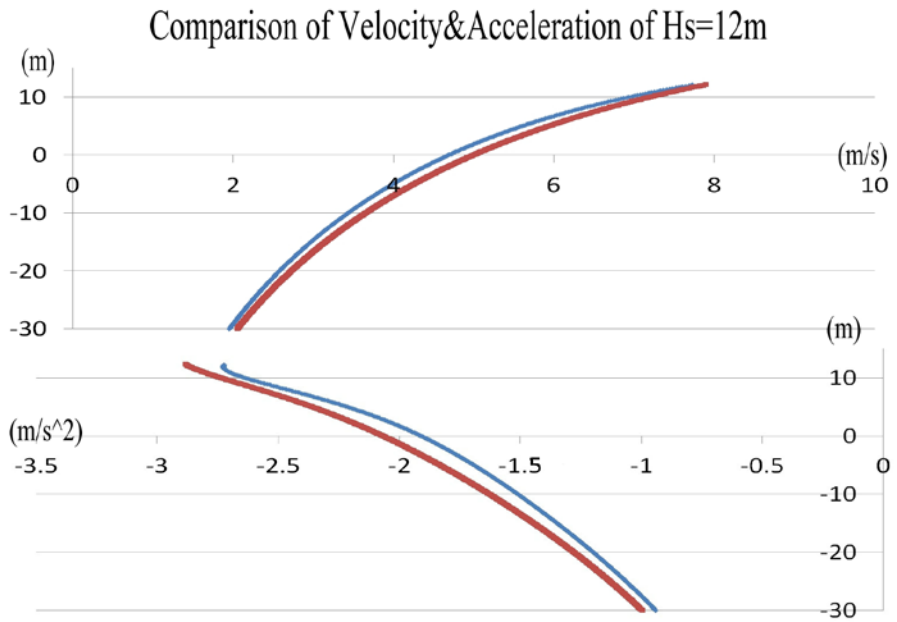

Figure15. Comparison of horiz.velocity and acceleration at the peak (Hs=12m).

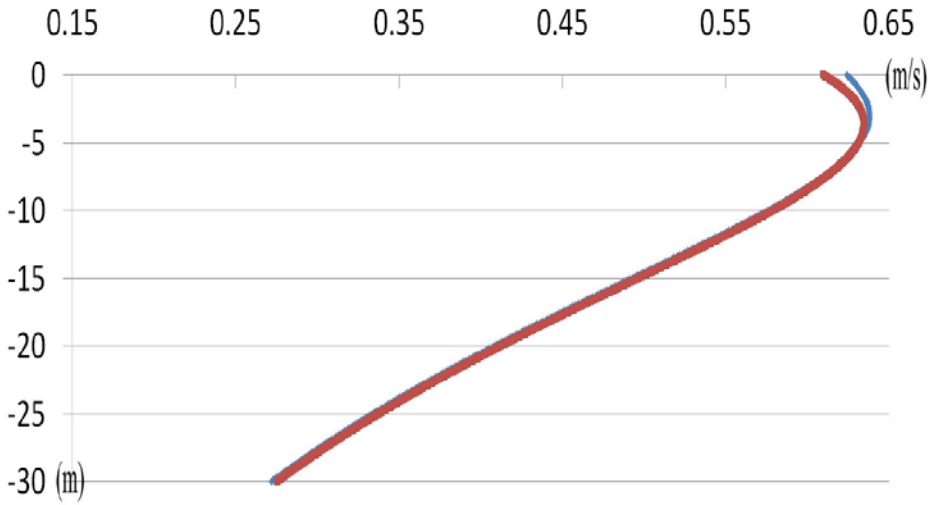

Figure 16. Comparison of vertical velocity at free surface (Hs=5m).

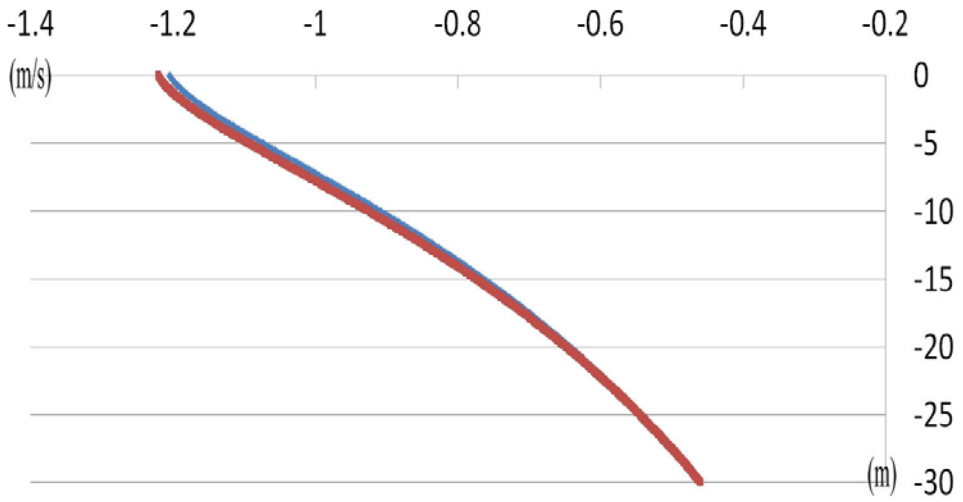

Figure 17. Comparison of vertical velocity at free surface (Hs=8m).

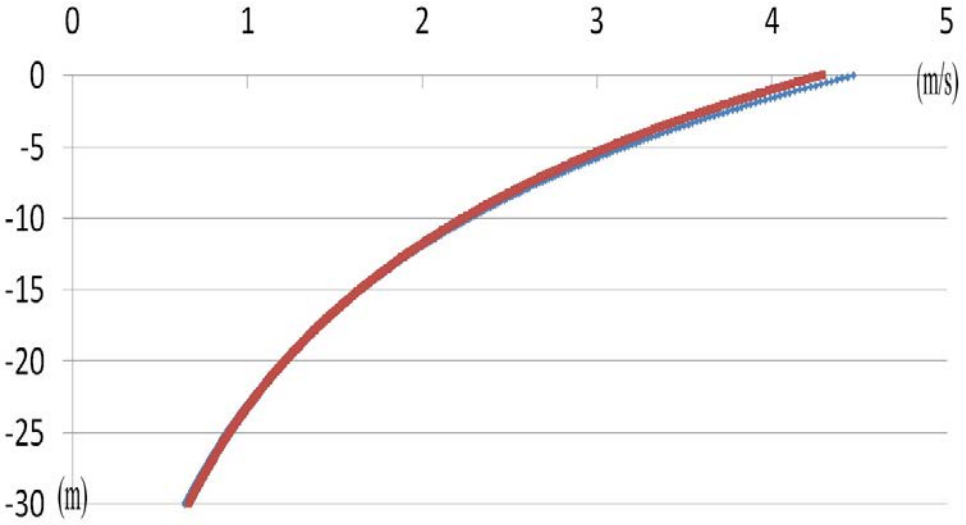

Figure 18. Comparison of vertical velocity at free surface (Hs=12m).

3.3 Discussion of a special case

During the study, such a result has been found that the shorter duration length of each segment, the shorter simulation time needed. But it is also found that as the duration length of segment goes shorter; the figure may not be recovered as well, especially when the wave is steep. Hence, a special case is discussed below.

Due to the maximum size of matrix (35*35) in the Matlab, plus the capability of current computer, the random seed can be only selected from 1 to 35 to produce the random number. (Neuman, 1996). During the research in this thesis, 20 different random seeds have been chosen to generate the rand (initial) phase. After comparing and analysis most of data, a special case is found which is the segment one of H_s=12m with random seed =12. As drawn in Figure 18, in both upper and lower profiles, from the comparison of peak regions, it is clear that they do not match very well. Plus, Figure 19 gives the comparison of horizontal velocity and vertical acceleration at the peak. It can be found that in the figure not only the wave elevation is distorted, but also is the kinematics.

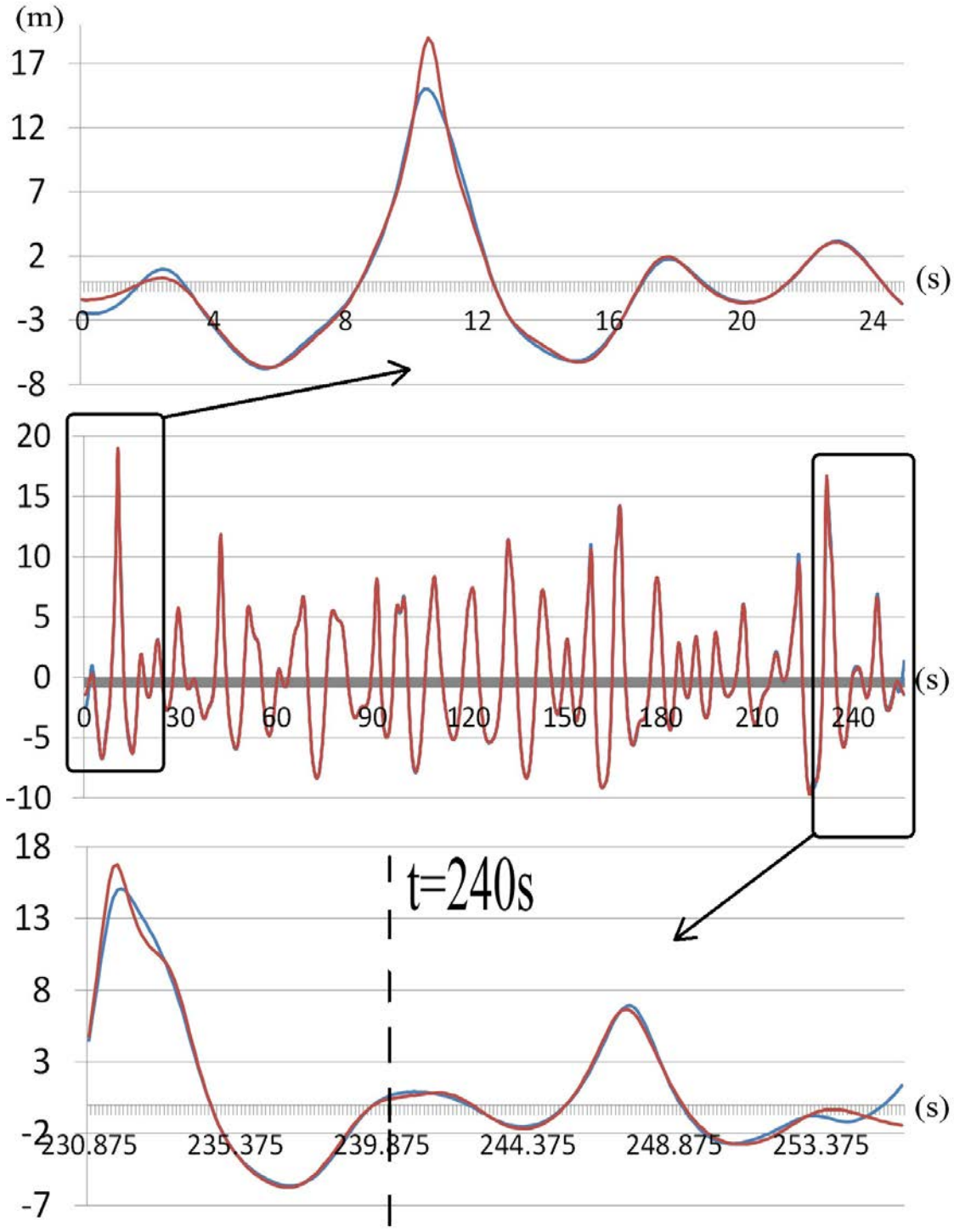

Figure 19. Comparison of wave elevations of segment 1 (Hs=12m).

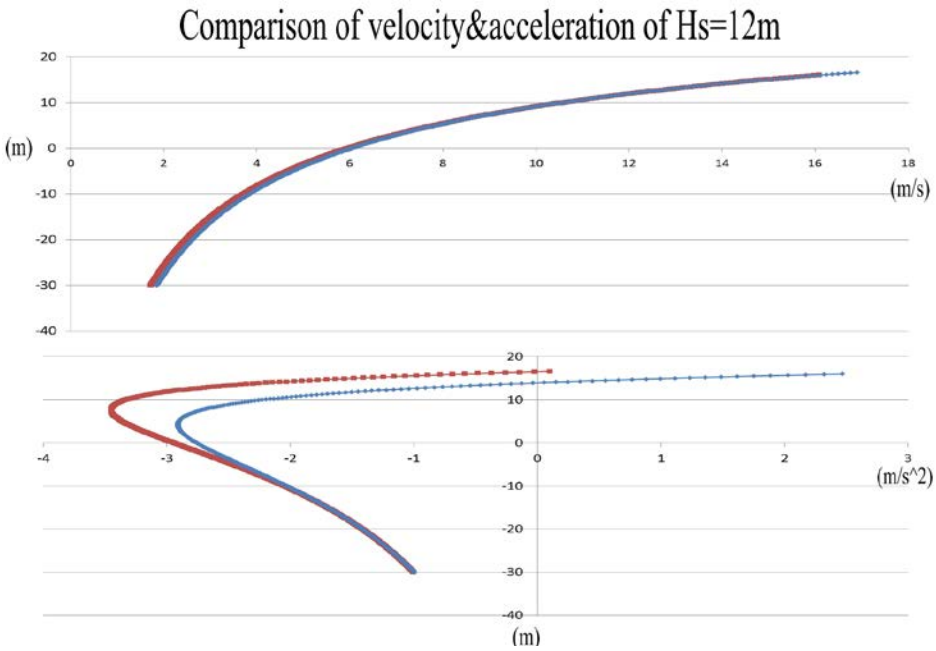

Figure 20. Comparison of horizontal velocity and acceleration at the peak (Hs=12m).

To avoid it, a test has been done by extending the length of segments in order to raise the number of components. Divide the wave elevation time series into five segments instead of nine and then the duration length of each segment becomes 512s rather than 256s. In such a way, the number of component doubled. Simulate the wave again and apply the effective overlap approach. The comparison of wave elevation profile of segment one under H_s=12m sea state is plotted in Figure 21. From comparison, it is clear that the profile of five-segment division fits the original wave elevation much better than the nine-segment division. Hence, to increase the duration length of each segment is an effective method when a distortion at the peak or tough exists during the simulation.

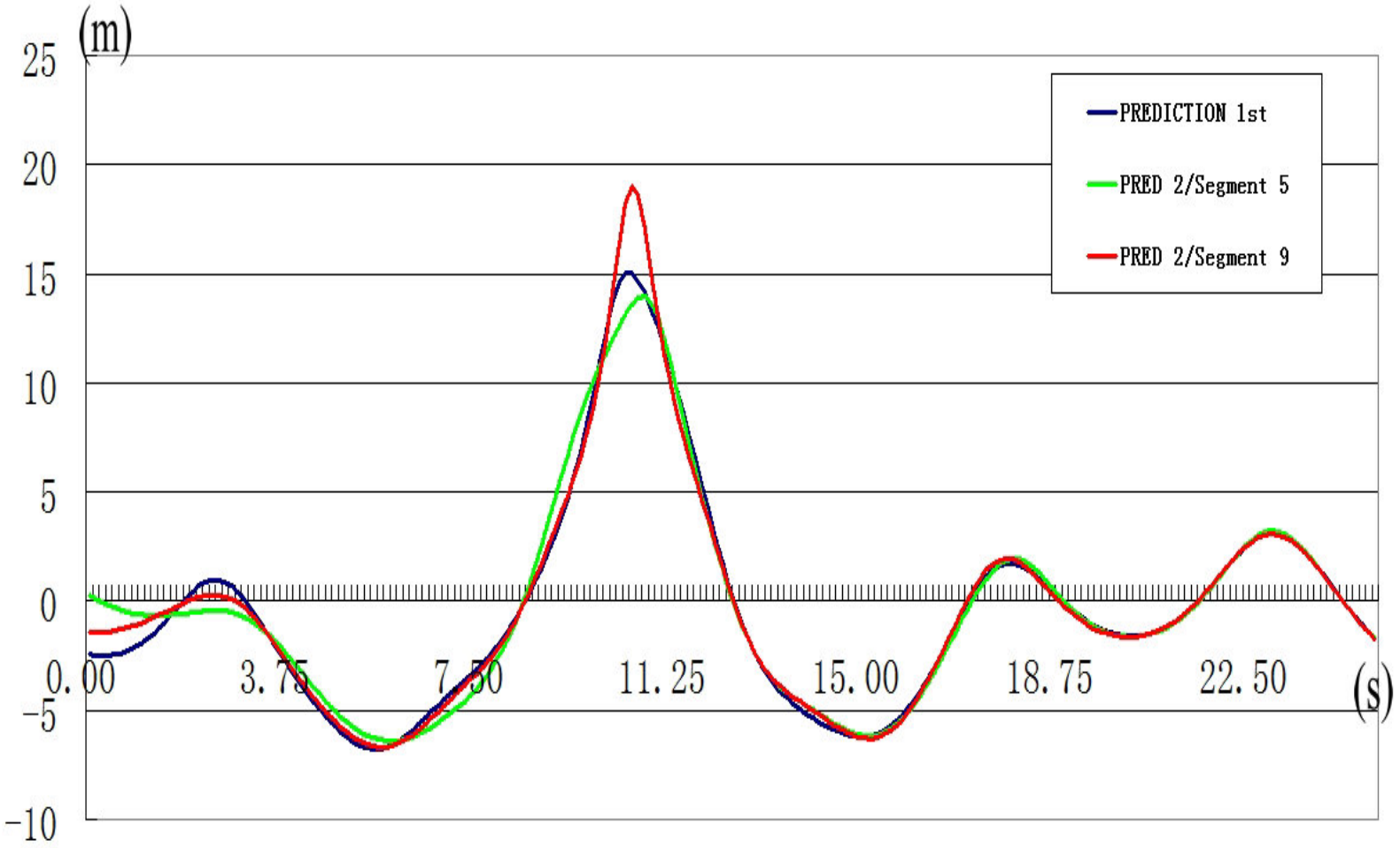

Figure 21. Comparison of wave segment 1 (Hs=12m).

4. APPLICATION

4.1 Introduction of application to COUPLE

Floating offshore wind turbines became a popular research topic nowadays and may become a vital choice for harnessing wind power in relatively deep water. Since the turbine interacts with the supporting floating hull, a coupled dynamic analysis is required to understand and quantify the interactions between the wind turbine, floating hull and its mooring system for the design. Related research was conducted on dynamic interactions between a wind turbines and its supporting floating structure. Shim (2007) and Bae, et al., (2011) integrated FAST-Charm3D to make uncoupled and coupled analysis on the TLP and Spar type floating wind turbines. Jonkman and Matha (2011) used FAST to investigate the dynamics of three types of platforms mentioned above. Masciola, et al. (2011) developed a FAST-OrcaFlex coupling code for the study of interactions between a wind turbine and its supporting Spar under the impact of periodic waves.

The numerical code, known as COUPLE, was developed and is continuously expanded and improved by his former and current graduate students and Professor Jun Zhang at Texas A&M University for the computation of the interaction between a floating structure and its mooring line/riser/tendon system in time domain. And it has been extended to collaborate with FAST for the simulation of the dynamic interaction. FAST was developed by the National Renewable Energy Laboratory (NREL) for computing the wind loads on a wind turbine. A 5MW wind turbine installed on the top of a classical Spar (Hywind-OC3 Spar) is employed to demonstrate the simulation. The

numerical results derived in this study may provide crucial information for the design of a floating wind turbine in the future.

The uniqueness in using COUPLE is that wave kinematics up to the free surface used in the Morison Equation is computed using a nonlinear deterministic Unidirectional Hybrid Wave Model (UHWM), and is at least accurate up to second order in wave steepness (Zhang et al., 1996; Spell et al., 1996). The advantage of the use of the UHWM, in addition to its accuracy there is no need to make choices among several empirical or stretching approximations, such as wheeler stretching and linear extrapolation (Peng et al., 2012). A non-repeated irregular wave simulation of a long duration (T) requires a very small frequency increment (1/T). As a result, the number of free wave components below the cut-off frequency will be extremely great. Because the UHWM used in COUPLE needs to calculate the wave interactions for every pair of free wave components, a large number of free wave components results in large CPU time. The total simulation duration of 3000s is divided into three segments and each is around 1100s with a 100s-ramp applied at the beginning (Peng, et al., 2012). While in the previous research, the model applied to simulate wave elevation in the COUPLE equivalently divide the wave segments, but it involves Gibbs phenomenon, respectively. Due to such discontinuity, sometimes we cannot obtain the convergent results from COUPLE. Applying the “Effective overlap approach”, the discontinuous region in each segment can be removed.

4.2 Characteristics of floating wind turbine model

Below are the test data comparing with paper (Peng et al., 2012) under the same initial condition and mooring model. Figure 22 is a sketch of Spar and its loading condition. Tables 4-7 gives wind turbine characteristics, met-ocean conditions, Hywind-OC3 Spar dimensions and mooring system properties, respectively.

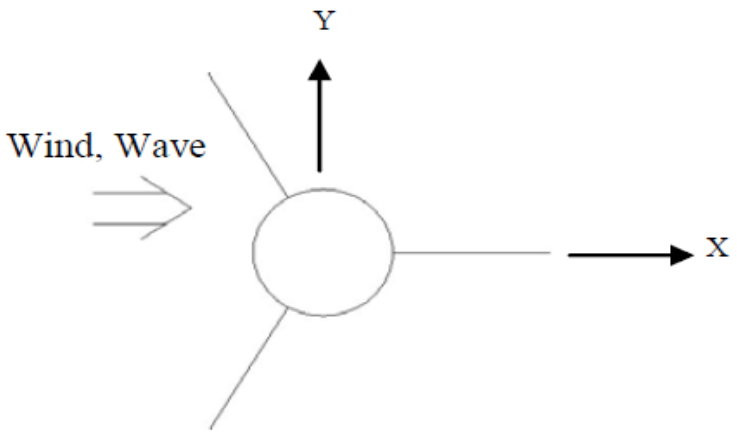

Figure 22. Sketch of Spar and loading conditions.

Table 3. Met-ocean conditions.

Reference Wind Speed at 10m height	13 m/s
Mean Wind Speed at Hub Height	17.11 m/s
Water Depth	320 m
Wave Heading	0 deg
Significant Wave Height	5.0 m
Peak Wave Period	8.69s

Table 4. NREL 5-MW wind turbine characteristics.

Rating	5 MW
Rotor orientation, configuration	Upwind, 3 blades
Rotor, hub diameter	126 m, 3 m
Hub height	90 m
Cut-in, rated, cut-out wind speed	3m/s, 11.4 m/s, 25 m/s
Cut-in, rated rotor speed	6.9 rpm, 12.1 rpm
Rated tip speed	80 m/s
Overhang, shaft tilt, precone	5 m, 5°, 2.5°
Rotor mass	110,000 kg
Nacelle mass	240,000 kg
Tower mass	249,718kg
Coordinate location of overall center of mass (CM)	(-0.2 m, 0.0 m, 64.0 m)

Table 5. Hywind-OC3 Spar dimensions.

Depth to Platform Base Below SWL (Total Draft)	120 m
Elevation to Platform Top (Tower Base) Above SWL	10 m
Depth to Top of Taper Below SWL	4 m
Depth to Bottom of Taper Below SWL	12 m
Platform Diameter Above Taper	6.5 m
Platform Diameter Below Taper	9.4 m
Platform Mass, Including Ballast	7,466,330 kg
CG Below SWL (Spar only)	89.9155 m
CG Below SWL (Spar and the wind turbine)	78.0018m
Platform Roll Inertia about CG	4,229,230,000 kg•m2
Platform Pitch Inertia about CG	4,229,230,000 kg•m2
Platform Yaw Inertia about Platform Centerline	164,230,000 kg•m2

Table 6. Mooring system properties.

Number of Mooring Lines	3
Angle Between Adjacent Lines	120°
Depth to Anchors Below SWL (Water Depth)	320 m
Depth to Fairleads Below SWL	70.0 m
Radius to Anchors from Platform Centerline	853.87 m
Radius to Fairleads from Platform Centerline	5.2 m

4.3 Numerical results and analysis

The numerical results include two parts. First, under the H_s=5m / T_p=10s condition, a simulation duration 1024s and dt=0.125s wave elevation time series is generated and its corresponding discrete amplitude spectrum is input the COUPLE to calculate the 6 DOF motions of the Spar. Then, divide such wave elevation time series into five segments, each simulation duration equals to 256s where we apply the "Effective overlap" approach. Similarly, input their corresponding discrete amplitude spectrum to COUPLE. The comparison of the 6 DOF motion at the CG (center of gravity) of the Spar is plotted in the Figure 23. In the figure, the motions that calculated by the original wave is plotted in the solid line and the motions calculated by wave segments is plotted in dash line. And also the comparison of their statistics is given in the Table 8. During the comparison of 6 DOF and their statistics, it is obvious that the

profiles are well matched. It is solid evidence that the results are consistent, after applying the “Effective overlap” approach.

The efficiency of the “Effective overlap” approach is discussed in the second part of the numerical results. The consistence has been tested in the first part, the efficiency which is the main task of the approach need to be tested, too. In the first part, the CPU time reduces from 2 hours minutes to 40 minutes in the calculation of COUPLE for a simulation duration 1024s and dt=0.125s wave elevation. Base on the theory, the longer wave it is, the more simulation time it saves, when apply the “Effective overlap” approach. Hence, a simulation duration 2048s and dt=0.125s wave elevation time series is tested as an example. In the previous research, using a Pentium (R) Dual-Core CPU T4500 @ 2.30GHz 2.29GHz 2.93GHz 2.93GB of RAM laptop, the CPU time of such time series is equal to around 16 hours. After applying the “Effective overlap” approach where we divide it into nine segments, the calculation time reduces to no more than two hours and a half. Plus, the results are still robust. Figures 24 and 25 are the 6 DOF at the CG of the Spar under the H_s=5m and 8m condition. And table 9 and 10 are their statistic details.

Table 7. Comparison of 6 DOF statistics (Top-original wave; Bottom-wave segmnets).

	Surge(m)	Sway(m)	Heave(m)	Roll(deg)	Pitch(deg)	Yaw(deg)
Max	11.73	0.36	0.14	0.60	5.64	1.49
Min	-0.01	-0.28	-0.39	-0.30	-0.01	-1.65
Mean	7.94	0.08	-0.13	0.15	3.26	-0.02
Std	2.54	0.13	0.11	0.15	1.03	0.45
Var	6.47	0.02	0.01	0.02	1.05	0.21

	Surge(m)	Sway(m)	Heave(m)	Roll(deg)	Pitch(deg)	Yaw(deg)
Max	11.85	0.35	0.19	0.60	5.57	1.49
Min	-0.01	-0.27	-0.51	-0.27	-0.01	-1.64
Mean	7.91	0.08	-0.13	0.15	3.25	-0.02
Std	2.59	0.13	0.14	0.15	1.04	0.45
Var	6.71	0.02	0.02	0.02	1.07	0.21

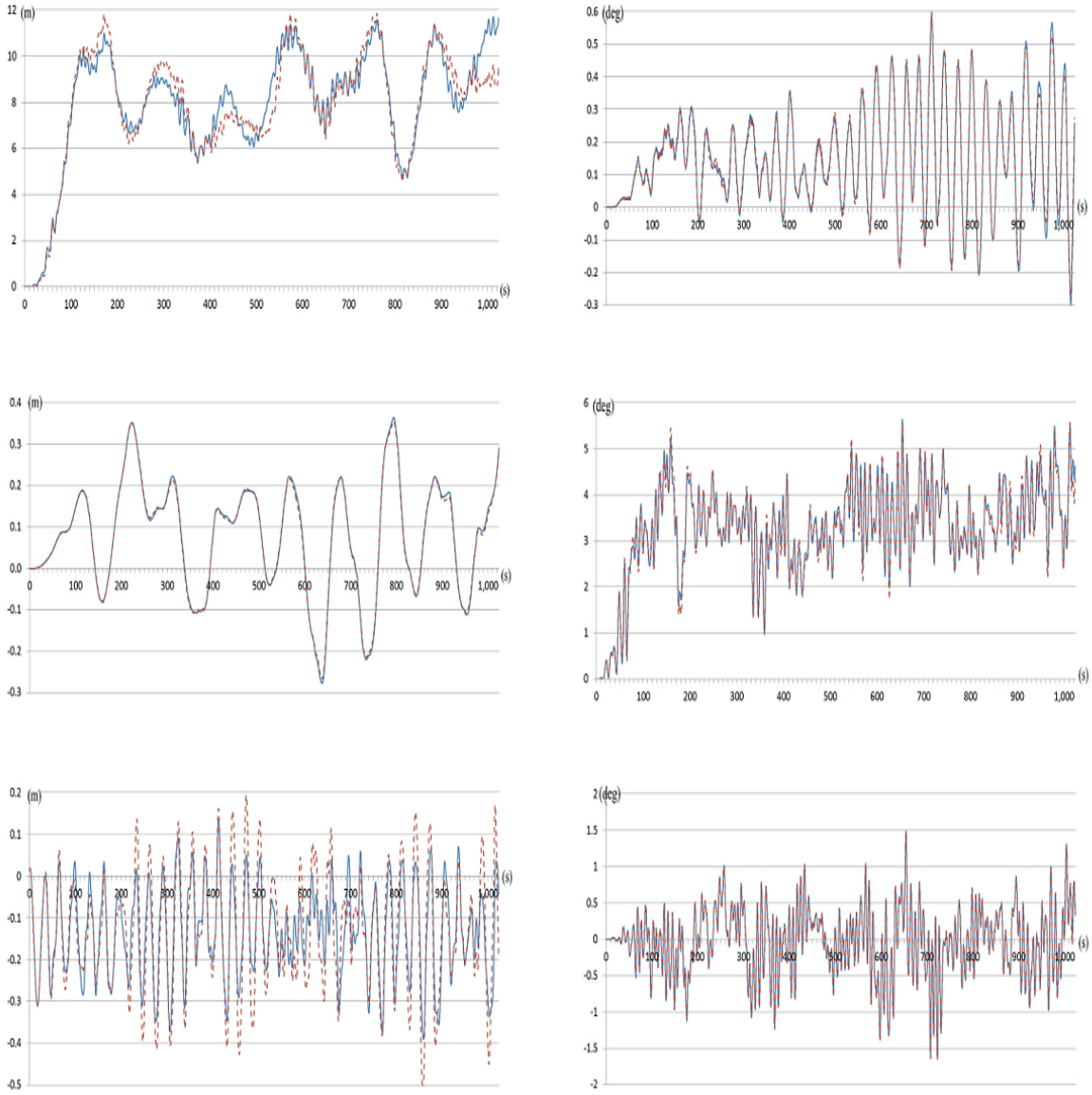

Figure 23. Comparison of 6 DOF motions of the Spar at the gravity center (Left: Top-Surge/Middle-Sway/Bottom-Heave; Right: Top-Roll/Middle-Pitch/Bottom-Yaw)

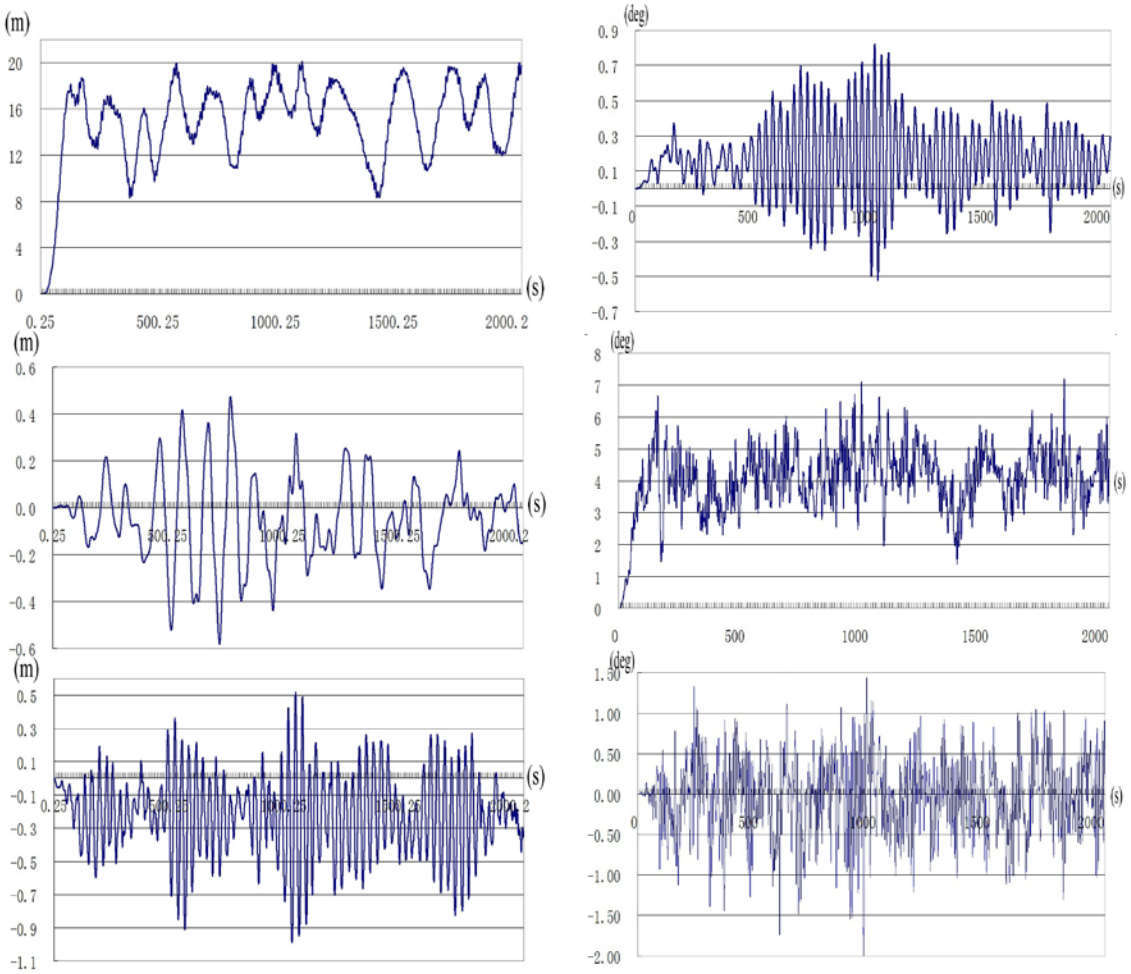

Figure 24. 6 DOF motions of the Spar at the gravity center (H_s=5m).

Table 8. Statistics of 6 DOF motions of the hull at CG (H_s=5m).

H_s=5m	Surge(m)	Sway(m)	Heave(m)	Roll(deg)	Pitch(deg)	Yaw(deg)
Max	20.136	0.473	0.518	0.802	7.219	1.432
Min	-0.012	-0.582	-0.990	-0.516	0.000	-2.063
Mean	14.891	-0.045	-0.220	0.172	4.068	-0.057
Std	3.719	0.181	0.246	0.229	1.031	0.458
Var	13.834	0.033	0.061	0.000	0.000	0.000

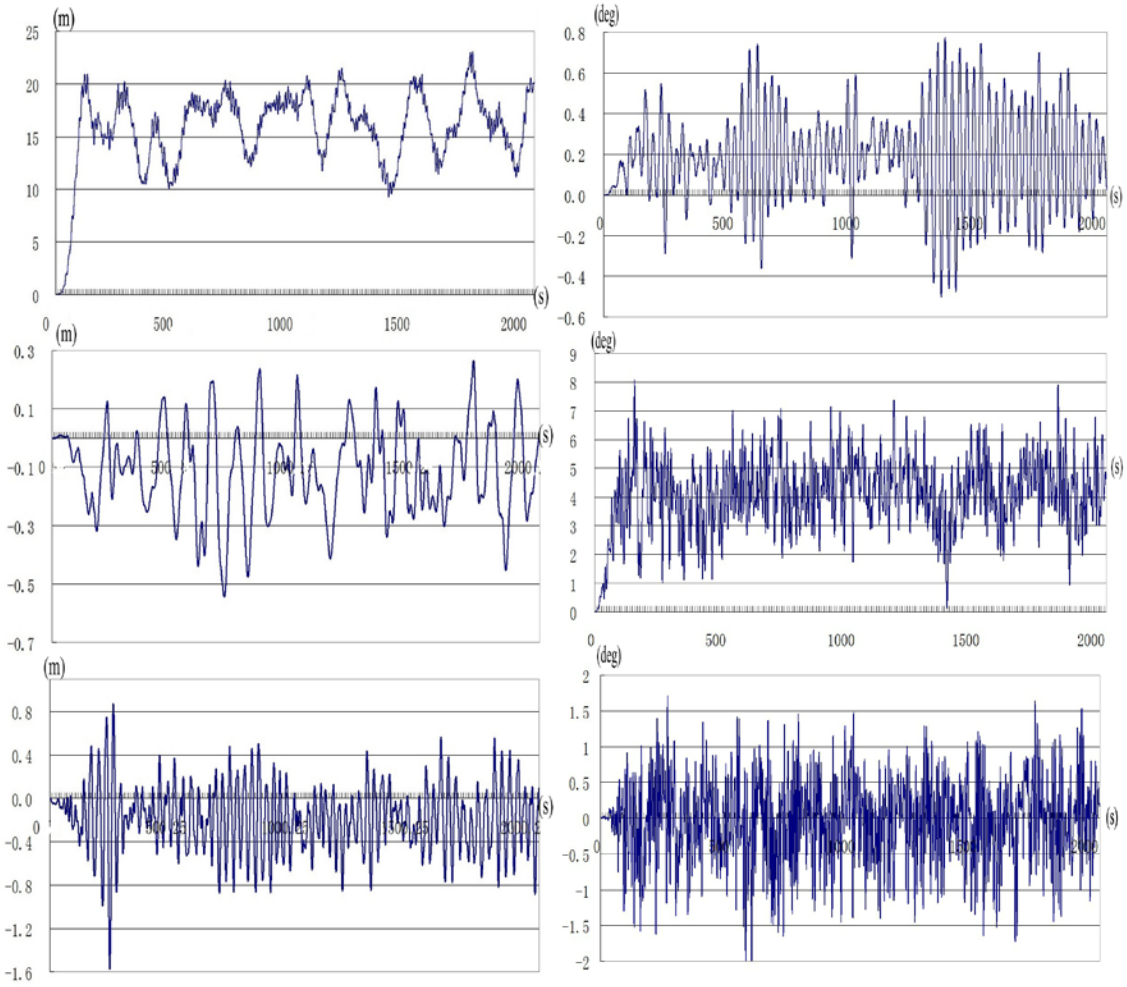

Figure 25. 6 DOF motions of the Spar at the gravity center (H_s=8m).

Table 9. Statistics of 6 DOF Motions of the hull at CG (H_s=8m).

H_s=8m/0deg	Surge(m)	Sway(m)	Heave(m)	Roll(deg)	Pitch(deg)	Yaw(deg)
Max	23.048	0.265	0.868	0.802	8.079	1.719
Min	-0.005	-0.542	-1.570	-0.516	0.000	-2.063
Mean	15.719	-0.112	-0.185	0.172	4.125	-0.057
Std	3.859	0.152	0.307	0.229	1.261	0.573
Var	14.896	0.023	0.094	0.000	0.057	0.000

5. SUMMARY

The Unidirectional Hybrid Wave Model (UHWM) allows accurate computation of irregular wave elevations, kinematics and wave induced pressure, which in turn allows accurate computation of wave loads on a slender body, such as Spar and TLP floating structures. Offshore industry usually requires 3-hour simulation of a floating structure impacted by severe ocean waves, in order to obtain meaningful statistics of motions of the platform and tensions in mooring lines and risers. Since the UHWM calculates nonlinear wave-wave interaction at least up to the second order in wave steepness, a long time duration (such as 3 hours) in general requires more free-wave components used in the simulation and dramatically increases the computation time of wave loads on the offshore structure. To reduce the CPU time, an efficient scheme has been developed in this thesis.

The input to the UHWM for calculating wave elevation, kinematics, and pressure can be either a measured wave property (such as wave elevation, kinematics and pressure recorded at a fixed location) or a wave spectrum of given a significant wave height (H_s) and a peak period (T_p) (such as JONSWAP) plus randomly selected initial phases assigned to the related free-wave components. In this study, the numerical scheme is described mainly based on the input of a wave spectrum, namely, JONSWAP. However, the scheme can be straightforwardly applied to the input as a measured time series of a wave property or the other types of wave spectra. The numerical scheme described in this study includes three main steps. The first is to modify the JONSWAP spectrum to eliminate the bound-wave (nonlinear) effects, mainly in the relatively high

frequency band. The second includes the discretization of an energy spectrum to obtain the amplitudes of the free-wave components, the assignment of a random initial phase to each free-wave component, and the use of PREDICTION in the UHWM to generate irregular surface wave elevations for a given simulation duration T, say 3 hours. The third step is to divide the 3-hour simulated time series of wave elevation into (N+1) segments of equal time length, where N is an integer power of 2. Then the DECOMPOSITION in the UHWM is applied to each segment of the wave elevation to obtain the amplitudes and initial phases of the free-wave components as a function of the frequency for that segment. Considering the number of total data points in a segment is M, the total number of data points in the simulation duration is NM. Thus, the N+1th segment allows an overlap between each pair of two consecutive (or neighboring) segments. The overlap duration hence has M/N data points. The overlap duration is necessary to remove the discontinuity at the beginning and end of each segment which results from the well known Gibbs phenomenon in the FFT, when these segments are used to simulate continuous irregular waves of long duration.

Three different sea states (mild, rough and severe) were simulated to demonstrate the capability and efficacy of the numerical scheme. It was found that the discontinuity resulting from the Gibbs phenomenon in the FFT can be removed by using overlap duration between two consecutive segments. The smooth transition between two consecutive segments is observed not only in wave elevation but also in wave kinematics, which are important in calculating wave loads on a slender structure.

Finally, the numerical scheme has been used in COUPLE to simulate the interaction among a moored Spar, its mooring system and a 5-MW wind turbine installed on the top of the Spar under the impact of wind, waves and currents. It is found that the CPU time is significantly reduced when the numerical scheme proposed in this study is adopted. In comparison with the same simulation but using the UHWM over the whole time duration instead of the division of segments, the CPU time for the 2048 seconds simulation of the floating wind farm is reduced from 16 hours to about 2.5 hours when the simulation was made on a Pentium (R) Dual-Core CPU T4500 @ 2.30GHz 2.29GHz 2.93GHz 2.93GB of RAM laptop.

REFERENCES

Bae, Y.H., Kim, M.H., Im, S.W., Chang, I.H., 2011. Aero-elastic-control-floater-mooring coupled dynamic analysis of floating offshore wind turbines. International offshore and polar engineering conference, Maui, Hawaii, USA. 2011.

Carslaw, H.S., 1930. Introduction to the theory of fourier's series and integrals (third edition). Chapter 4, 271–276. Dover Publications, 3rd Revised & Enlarged edition, New York.

Goda, Y., 1987. Standard spectra and statistics of sea waves derived by numerical simulation. Proceedings of the 34th Japan conference on coastal engineering, pp. 131-135.

Jonkman, J.M., Matha, D., 2011. Dynamics of offshore floating wind turbines – analysis of three concepts". Wind Energy, Vol. 14, 557–569.

Masciola, M., Robertson, A., Jonkman, J.M., Driscoll, F., 2011. Investigation of a FAST-OrcaFlex coupling module for integrating turbine and mooring dynamics of offshore floating wind turbines. International conference on offshore wind energy and ocean energy, Beijing, China. 2011.

Neuman, E., 1996. Using Matlab in linear algebra. Tutorial 3 (Math221), 20-26. Department of Mathematics, Southern Illinois University at Carbondale1, 1996. http://www.math.siu.edu/matlab/tutorial3.pdf

Peng, C., Yan, F.S., Zhang, J., 2012. Coupled dynamic analysis of a floating offshore wind turbine. Proceedings of the 17th Offshore Symposium, Section C, February 2, 2012, Houston, Texas, USA.

Rössel, J. 2010. Personal own work, drawn with Inkscape's function plotter, Wikipedia. http://en.wikipedia.org/wiki/Gibbs_phenomenon

Shim, S., 2007. Coupled dynamic analysis of floating offshore wind farms. M.S.D. Dissertation, Texas A&M University, College Station.

Spell, C.A., Zhang, J., Randall, R.E., 1996. Hybrid wave model for unidirectional irregular waves, part II. comparison with laboratory measurements. Applied Ocean Research, Vol. 18, 93-110.

Stewart, R.H., 2005. Introduction to physical oceanography. Chapter 16: 287-288. Department of Oceanography, Texas A&M University. 2005. http://oceanworld.tamu.edu/resources/ocng_textbook/PDF_files/book_pdf_files.html

Zhang, J., Chen, L., Ye, M., Randall, R.E., 1996. Hybrid wave model for unidirectional irregular waves-part I. Theory and numerical scheme. Applied Ocean Research, Vol. 18, 77-92.

Zhang, J., Hong, K., Yue, D.K.P., 1993. Effects of wave length ratio on wave modeling. J. Fluid Mech, Vol. 248, 107-127.

APPENDIX A

JONSWAP spectrum modification

```
clear all;
close all;
clc;

%JONSWAP spectrum initial data
NSIZE=2048;
Hs=5.0;
Tp=10.0;
g=9.8065;
fp=1.0/Tp;
df=1/NSIZE;
gamma=3.3;
betaj=0.06238/(0.23+0.0336*gamma-0.185*(1.9+gamma)^-1)*(1.094-
0.01915*log(gamma));

%change seed of random functon if different random number is needed or else the
random number will be the same;
rand('state',8);
Ran=rand(NSIZE,1);
angle=2*pi*(Ran-0.5);

%Cutoff frequency is related to the Peak time
TCUT=Tp/3;
NCUT=fix(NSIZE/TCUT);
%NCUT=1112;
%NCUT can be fixed to a exact number if the prior sentence can not find a good enough
point as designed

%modifiy coefficient
alpha=0.45;

%WAVE STEEPNESS: if wave steepness(Hs*Kp) less than 0.1, then the nonlinear
effect hardly play roles, so we can neglect it and set CM=0;
k=4*pi^2/(g*Tp^2);
epsilon=(Hs*k)^2;
if epsilon<0.05;
   CM=0;
  Else
```

```
%Spectrum Modifiy Coefficient CM
CM=alpha*((Hs^2/Tp^4)*(16*pi^4/g^2)*Tp/TCUT);
end
%open a file to write the amplitude spectrum data
fid=fopen('free.dat','w');
tskip=0;
wdepth=1000;
amean=0.100000000000000E-010;
para=[tskip,wdepth,amean];
fprintf(fid,'    %15.13f        %15.12f      %16.15E\n',para);

%standard division format of the amplitude spectra is 81/281/421/615/920 for Hs=5m
Tp=10s case
%72/240/392/559/840 for Hs=8m Tp=11s case
%64/208/366/512/768 for Hs=12m Tp=12s case
ilow=80+1;
ilong=280+1;
isht=420+1;
iend=614+1;
%NOTE: In the Decompositon program, besides these four bourndry points, there is
another data called "tail band" should be input
%and so-called "tail band" ranges from the next point to the "iend" in the short wave
band 2 to cutoff frequency point or even
%lower depending on the certain case;

id=[ilow,ilong,isht,iend];
fprintf(fid,'%12d %11d %11d %11d\n',id);

fprintf(fid,' FREE.DAT\n');
fprintf(fid,'  FREE WAVE COMPONENTS OBTAINED FROM JONSWAP
SPECTRAM\n');
fprintf(fid,'\n');
fprintf(fid,'  FREQUENCY(HZ)  AMPLITUDE(M)    PHASE(RAD)\n');

f=zeros(NSIZE,1);
E=zeros(NCUT,1);
S=zeros(NSIZE,1);
SS=zeros(NSIZE,1);
a=zeros(NSIZE,1);
aa=zeros(NSIZE,1);

e=df:df:(NCUT*df);
for j=1:NCUT;
   if(e(j)<=fp)
```

```
    sigma=0.07;
   else
    sigma=0.09;
   end;
   d=exp(-(e(j)/fp-1)^2/2*(sigma^2));
   E(j)=betaj*Hs^2*Tp^-4*e(j)^-5*exp(-5/4*(Tp*e(j))^-4)*gamma^d;
end
z1=trapz(e,E);

%the iteration below is to find out the loation of the peak component l;
for k=1:(NCUT-1);
   if E(k)-E(k+1)<0;
      l=k+1;
   else
      m=k;
   end
end

%this modification number is related to the location of peak component, we choose 1.35
times larger than peak;
%NMODIF=ceil(1.35*l);
NMODIF=519;

%Modified spectrum Part.1 is the same as orginal;
for m=1:NMODIF;
   f(m)=m*df;
   if(f<=fp)
    sigma=0.07;
   else
    sigma=0.09;
   end;
   d=exp(-(f(m)/fp-1)^2/2*(sigma^2));
   S(m)=betaj*Hs^2*Tp^-4*f(m)^-5*exp(-5/4*(Tp*f(m))^-4)*gamma^d;
   SS(m)=S(m);
   a(m)=sqrt(2*SS(m)*df);
   aa(m)=a(m);
   fprintf(fid,' %15.6E %14.6E %14.6E\n',[f(m),aa(m),angle(m)]);
end
%Modified spectrum Part.2 is allpied by the CM coefficeint
for n=(NMODIF+1):NCUT;
 f(n)=n*df;
   if(f<=fp)
    sigma=0.07;
   else
```

```
     sigma=0.09;
   end;
   d=exp(-(f(n)/fp-1)^2/2*(sigma^2));
   S(n)=betaj*Hs^2*Tp^-4*f(n)^-5*exp(-5/4*(Tp*f(n))^-4)*gamma^d;
   a(n)=sqrt(2*S(n)*df);
   aa(n)=a(n)*(1-CM*(n-NMODIF-1)/(NCUT-NMODIF-1));
   SS(n)=aa(n)^2/2/df;
   fprintf(fid,' %15.6E %14.6E %14.6E\n',[f(n),aa(n),angle(n)]);
end
%Modified spectrum Part.3 is set to very small value, almost zero;
for p=(NCUT+1):NSIZE;
   f(p)=p*df;
   S(p)=betaj*Hs^2*Tp^-4*f(p)^-5*exp(-5/4*(Tp*f(p))^-4)*gamma^d;
   a(p)=sqrt(2*S(p)*df);
   aa(p)=0.1E-08;
   SS(p)=aa(p)^2/2/df;
   fprintf(fid,' %15.6E %14.6E %14.6E\n',[f(p),aa(p),angle(p)]);
end
z2=trapz(f,SS);
fclose(fid);

% figure(1)
% plot(f,S)
% %axis([0,0.5,0,45])
% title('Amplitude spectrum from MATLAB df=1/2048')
% xlabel('frequency (Hz)')
% ylabel('amplitude (m)')
%
% figure(2)
% plot(f,SS)
% %axis([0,0.5,0,45])
% title('MODIFIED Amplitude spectrum from MATLAB df=1/2048')
% xlabel('frequency (Hz)')
% ylabel('amplitude (m)')
```

APPENDIX B

Wave segment division

```
clear all;
close all;
clc;

%initial numbers

%the number of sectiontions
section=8;
T=2048;

%dt=time step
dt=1/8;
%total elevation points
total=T/dt;
%total points in each sectiontion
N=(T/section/dt);

aa=zeros(total,1);
time=zeros(total,1);
ee=zeros(total,1);

%each sectiontion has one elev? to record the elevation data;
elev=zeros(T/section,1);

load PELEVAT.DAT;     %input the wave elevation file with nonlinear interaction from
PREDICTION
aa=PELEVAT( :,2);    %read the amplitude of the wave elevation

for i=1:section+1
   fout=strcat('re',num2str(i),'.dat');
   fid=fopen(fout,'w');
   for m=1:1:N;
      if (i==1)
         n=m;
         else
         n=m+(N-N/section)*(i-1);
      end
      elev(m)=aa(n);
      fprintf(fid,' %14.6E %14.6E\n',[n*dt,elev(m)]);
```

```
    end
    fclose(fid);
end
```